

## Soil Moisture Memory in AGCM Simulations: Analysis of Global Land–Atmosphere Coupling Experiment (GLACE) Data

SONIA I. SENEVIRATNE,<sup>a,b,\*</sup> RANDAL D. KOSTER,<sup>a</sup> ZHICHANG GUO,<sup>c</sup> PAUL A. DIRMEYER,<sup>c</sup>  
EVA KOWALCZYK,<sup>d</sup> DAVID LAWRENCE,<sup>e</sup> PING LIU,<sup>f</sup> CHENG-HSUAN LU,<sup>g</sup> DAVID MOCKO,<sup>f</sup>  
KEITH W. OLESON,<sup>h</sup> AND DIANA VERSEGHY<sup>i</sup>

<sup>a</sup>Global Modeling and Assimilation Office, NASA Goddard Space Flight Center, Greenbelt, Maryland

<sup>b</sup>Goddard Earth Sciences and Technology Center, University of Maryland, Baltimore County, Baltimore, Maryland

<sup>c</sup>Center for Ocean–Land–Atmosphere Studies, Calverton, Maryland

<sup>d</sup>CSIRO Atmospheric Research, Aspendale, Victoria, Australia

<sup>e</sup>University of Reading, Reading, Berkshire, United Kingdom

<sup>f</sup>Science Applications International Corporation, Beltsville, Maryland

<sup>g</sup>National Centers for Environmental Prediction, Camps Springs, Maryland

<sup>h</sup>National Center for Atmospheric Research, <sup>+</sup> Boulder, Colorado

<sup>i</sup>Meteorological Service of Canada, Toronto, Ontario, Canada

(Manuscript received 14 December 2004, in final form 6 January 2006)

### ABSTRACT

Soil moisture memory is a key aspect of land–atmosphere interaction and has major implications for seasonal forecasting. Because of a severe lack of soil moisture observations on most continents, existing analyses of global-scale soil moisture memory have relied previously on atmospheric general circulation model (AGCM) experiments, with derived conclusions that are probably model dependent. The present study is the first survey examining and contrasting global-scale (near) monthly soil moisture memory characteristics across a broad range of AGCMs. The investigated simulations, performed with eight different AGCMs, were generated as part of the Global Land–Atmosphere Coupling Experiment.

Overall, the AGCMs present relatively similar global patterns of soil moisture memory. Outliers are generally characterized by anomalous water-holding capacity or biases in radiation forcing. Water-holding capacity is highly variable among the analyzed AGCMs and is the main factor responsible for intermodel differences in soil moisture memory. Therefore, further studies on this topic should focus on the accurate characterization of this parameter for present AGCMs. Despite the range in the AGCMs' behavior, the average soil moisture memory characteristics of the models appear realistic when compared to available in situ soil moisture observations. An analysis of the processes controlling soil moisture memory in the AGCMs demonstrates that it is mostly controlled by two effects: evaporation's sensitivity to soil moisture, which increases with decreasing soil moisture content, and runoff's sensitivity to soil moisture, which increases with increasing soil moisture content. Soil moisture memory is highest in regions of medium soil moisture content, where both effects are small.

### 1. Introduction

Soil moisture memory, in essence the fact that the soil can “remember” a wet or dry anomaly long after

\* Current affiliation: Institute for Atmospheric and Climate Science, ETH Zurich, Zurich, Switzerland.

<sup>+</sup> The National Center for Atmospheric Research is sponsored by the National Science Foundation.

Corresponding author address: Dr. Sonia Seneviratne, Institute for Atmospheric and Climate Science, ETH Zurich, Universitätsstrasse 16, 8092 Zurich, Switzerland.  
E-mail: sonia.seneviratne@env.ethz.ch

the conditions responsible for the anomaly are forgotten by the atmosphere, is a key aspect of land–atmosphere interactions and has major implications for seasonal forecasting. Indeed, due to its inherent memory, soil moisture is one of the major “slow” drivers of the climate system and possibly the chief source of forecast skill for summer precipitation over land in the midlatitudes (Koster et al. 2000). A detailed understanding of the processes controlling soil moisture memory is therefore necessary for assessing the predictability associated with soil moisture on subseasonal to seasonal time scales, and for characterizing important mechanisms impacting land–atmosphere interactions on these scales.

Various studies have investigated soil moisture memory characteristics either from observations (e.g., Vinnikov and Yeserkepova 1991; Vinnikov et al. 1996; Entin et al. 2000; Wu et al. 2002) or from integrations with land surface models (LSMs) or atmospheric general circulation models (AGCMs; e.g., Delworth and Manabe 1988; Liu and Avissar 1999a; Koster and Suarez 2001; Schlosser and Milly 2002; Mahanama and Koster 2003; Wu and Dickinson 2004). The observational studies, necessarily bound in scope by the limited spatial and temporal availability of the soil moisture measurements and by the lack of observations of evaporation, have generally focused on the analysis of anomaly decay time scales for local soil moisture observations, combined in some cases with inferences from simple analytical models (e.g., Liu and Avissar 1999b; Albertson and Kiely 2001). The modeling studies, taking advantage of the extensive data available from comprehensive model simulations, have focused instead on a more global and detailed understanding of the processes controlling soil moisture memory in the framework of a given AGCM or LSM with the caveat of the possible model dependency of the results obtained. A way to address the issue of model dependency is to analyze such properties for a number of models in a common framework and to thereby establish the effects of specific model characteristics and biases on the simulated soil moisture memory. This is the main purpose of the present study.

This investigation is the first survey examining and contrasting soil moisture memory characteristics across a broad range of AGCMs. The investigated simulations—16-member ensembles spanning 1 June to 31 August for eight different AGCMs—were generated as part of the Global Land–Atmosphere Coupling Experiment (GLACE; Koster et al. 2004a, 2006; Guo et al. 2006). For the analysis of the simulations, we use an approach proposed by Koster and Suarez (2001, hereafter referred to as KS01) that relates soil moisture autocorrelation within a climate model to various climatic and model characteristics. This allows us to relate the simulated soil moisture memory within each AGCM to its representation of specific physical processes and feedback mechanisms.

The structure of the paper is as follows. Section 2 describes the analysis framework of this study (model data and the KS01 soil moisture memory equation). Section 3 gives a brief evaluation of the atmospheric forcing generated in the analyzed simulations, as well as a description of mean climatic and hydrological characteristics of the AGCMs. Section 4 describes the overall soil moisture memory characteristics of the AGCMs, and section 5 presents an analysis of the AGCMs' soil

moisture memory using the KS01 framework. Then, section 6 discusses the dependence of soil moisture memory on the soil moisture regime, and section 7 presents a brief combined evaluation of soil moisture memory and land–atmosphere coupling in the perspective of soil moisture initialization for seasonal forecasting. Finally, the main conclusions are given in section 8.

## 2. Analysis framework

### a. Employed data from GLACE

The analyzed simulations are taken from GLACE, a recent project investigating the strength of land–atmosphere coupling in AGCMs. As part of this experiment, three ensembles of simulations spanning 1 June–31 August were conducted by a number of different AGCMs, using different specifications for the land–atmosphere coupling (full coupling, partial coupling, and no coupling). In the present study, we investigate the soil moisture characteristics of the control experiments (with full coupling, i.e., “ensemble W”) for eight of the participating AGCMs: Community Atmospheric Model version 3 (CAM3), Canadian Centre for Climate Modelling and Analysis (CCCma), Commonwealth Scientific and Industrial Research Organisation Conformal Cubic version 3 (CSIRO-CC3), Center for Ocean–Land–Atmosphere (COLA), AGCM used in the Climate and Radiation Branch at the National Aeronautics and Space Administration Goddard Space Flight Center (NASA GSFC) (GEOS-CRB), Hadley Centre Atmospheric Model version 3 (HadAM3), National Centers for Environmental Prediction (NCEP) Global Forecast System (GFS), and NASA Seasonal-to-Interannual Prediction Project (NSIPP). The main characteristics of these eight AGCMs are detailed in Tables 1 and 2). Some GLACE models are excluded from this study because they did not provide the full complement of necessary data for our calculations.

The analyzed ensemble, consisting of 16 members differing only in their initialization, is essentially a standard set of AGCM simulations with prescribed sea surface temperature (SST). The SST boundary conditions for the integrations are the observed conditions in 1994, a year not characterized by either El Niño or La Niña conditions. Note then that the impact of interannually varying SSTs on soil moisture memory, which can be particularly strong in the Tropics (Koster et al. 2000), is not analyzed in this study. For the initialization of the ensemble simulations, GLACE participants were provided with various approaches that ensured that the initial conditions would not be artificially similar between the ensemble members. The soil wetness fields analyzed here were computed in a consistent way for all

TABLE 1. AGCM–LSM combinations corresponding to the simulations analyzed in this paper.

Model	Resolution	General LSM characteristics
CAM3 (Collins et al. 2004; Bonan et al. 2002; Oleson et al. 2004)	T42, $2.8^\circ \times 2.8^\circ$	Community Land Model version 3 (CLM3). Complete water and energy budget. Impact of vegetation is explicitly parameterized. Subgrid-scale processes are accounted.
CCCma (McFarlane et al. 1992; Boer et al. 1992; Verseghy 1991)	T32, $3.75^\circ \times 3.75^\circ$	Canadian Land Surface Scheme (CLASS). Complete water and energy budget. Impact of vegetation is explicitly parameterized.
COLA (Kinter et al. 1997; Xue et al. 1991; Dirmeyer and Zeng 1999)	T63, $1.875^\circ \times 1.875^\circ$	Simplified Simple Biosphere model (SSiB). Complete water and energy budget. Impact of vegetation is explicitly parameterized.
CSIRO-CC3 (McGregor and Dix 2001; McGregor 1996; Kowalczyk et al. 1994)	$2^\circ \times 2^\circ$	Soil-canopy scheme. Complete water and energy budget. Impact of vegetation is explicitly parameterized. Subgrid-scale processes are accounted.
GEOS-CRB (Conaty et al. 2001; Sud and Walker 1999a,b; Mocko and Sud 2001)	$2.5^\circ \times 2^\circ$	HY-SSiB (a version of SSiB). Complete water and energy budget. Impact of vegetation is explicitly parameterized.
HadAM3 (Pope et al. 2000; Cox et al. 1999; Essery et al. 2003)	$3.75^\circ \times 2.5^\circ$	MOSES2. Complete water and energy budget. Impact of vegetation is explicitly parameterized. Subgrid-scale processes are accounted.
NCEP GFS (Kalnay et al. 1996; Moorthi et al. 2001; Pan and Mahrt 1987)	T62, $1.875^\circ \times 1.875^\circ$	Oregon State University (OSU) LSM. Complete water and energy budget. Impact of vegetation is explicitly parameterized.
NSIPP (Bacmeister et al. 2000; Koster and Suarez 1992, 1996)	$2.5^\circ \times 2^\circ$	Mosaic LSM. Complete water and energy budget. Impact of vegetation is explicitly parameterized.

AGCMs, as the vertically integrated soil moisture above the wilting point divided by the maximum allowable soil moisture above the wilting point. For a more detailed description of the experimental design and the analysis of AGCMs' land–atmosphere coupling strength, please refer to Koster et al. (2004a, 2006) and Guo et al. (2006).

### b. Soil moisture autocorrelation equation

Delworth and Manabe (1988) pioneered the study of soil moisture memory in AGCMs, using a first-order Markov process model to relate memory to potential evaporation and soil water-holding capacity. KS01 provide a more comprehensive equation that relates soil moisture autocorrelation to several features of the investigated model, including the sensitivity of runoff to soil moisture, land–atmosphere feedbacks, and seasonality. Note that under various simplifying assumptions (e.g., assuming that soil moisture memory is mostly controlled by evapotranspiration) the equation simplifies to the result of Delworth and Manabe (1988). The derivation of the KS01 soil moisture autocorrelation equation is briefly presented in this subsection. Please refer to KS01 for a more detailed description.

KS01 assume that the water balance for the soil column of a typical LSM, for the time period  $[n, n + 1]$  (e.g., month) of year<sup>1</sup>  $y$ , can be written (in the absence of snow) as

$$C_s w_{n+1,y} = C_s w_{n,y} + P_{n,y} - E_{n,y} - Q_{n,y}, \quad (1)$$

where  $C_s$  is the column's water-holding capacity,  $w_n$  ("soil wetness") is the average degree of saturation in the column as a whole [value at the beginning of time period  $(n, n + 1)$ ],  $P$  is precipitation,  $E$  is the total evaporation (i.e., transpiration, bare soil evaporation, and interception loss), and  $Q$  is the total runoff (including both surface and subsurface runoff). Here  $P_{n,y}$ ,  $E_{n,y}$ , and  $Q_{n,y}$  are accumulated fluxes during the time period  $(n, n + 1)$ .

Following the approach of Koster and Milly (1997), KS01 approximate the dependence of scaled evaporation and runoff on soil moisture with simple empirically fitted linear functions:

$$\frac{Q_{n,y}}{P_{n,y}} = a \left( \frac{w_{n,y} + w_{n+1,y}}{2} \right) + b, \quad \text{and} \quad (2)$$

$$\frac{E_{n,y}}{R_{n,y}} = c \left( \frac{w_{n,y} + w_{n+1,y}}{2} \right) + d. \quad (3)$$

In the above equation,  $R_{n,y}$  is the accumulated net radiation during the time period  $(n, n + 1)$  (normalized by the latent heat of vaporization, to have the same units as  $E$ ); note that  $R_{n,y}$  is used instead of potential evaporation for the normalization of actual evaporation due to the lack of information about potential evaporation from the models and even its proper definition (KS01). The empirically derived, model-specific parameters  $a$ ,  $b$ ,  $c$ , and  $d$  are established for each AGCM and at each grid point through analysis of the simulations.

Equations (2) and (3) are substituted into (1). Then, by separating  $w$ ,  $P$ , and  $R$  into their mean components

<sup>1</sup> For the present study,  $y$  corresponds to each ensemble member.

TABLE 2. LSM characteristics of the AGCMs analyzed in this paper;  $C_s$  refers to the water-holding capacity.

Model	Total soil depth	Active soil depth	$C_s$	Field capacity	Wilting point	Layer discretization
CAM3	3.43 m	Root distribution varying by plant functional type	Saturation water content	Not defined	$-1.5 (10^5)$ mm for all plant functional types (matrix potential)	Ten layers defined at node depths of 0.0071, 0.0279, 0.0623, 0.1189, 0.2122, 0.3661, 0.6198, 1.0380, 1.7276, and 2.8646 m
CCCma	4.1 m	Spatially varying max rooting depth [Food and Agricultural Organization United Nations Educational, Scientific, and Cultural Organization (FAO-UNESCO) soil maps]	Saturation water content	Function of soil texture	Function of soil texture	Three layers: 10 cm, 25 cm, and 3.75 m thick
COLA	Based on International Satellite Land Surface Climatology Project (ISLSCP) I-1 CD-ROM	Function of vegetation type and total soil depth	Saturation water content	Function of soil type	Function of soil and vegetation types	Three layers: surface layer is 5 cm globally; depth of root and recharge layers are functions of vegetation type and total soil depth
CSIRO-CC3	4.6 m	Up to 1.728 m (root distribution by layers: 0.05, 0.1, 0.35, 0.4, 0.1, and 0.0)	Saturation water content	Function of soil type (Zobler 1986)	Function of soil type (Zobler 1986)	Six layers: 0.022, 0.058, 0.154, 0.409, 1.085, and 2.872 m thick
GEOS-CRB	Function of vegetation type	Function of vegetation type	Saturation water content	Function of vegetation type	Function of vegetation type	Three layers (surface, root zone, and deep recharge layers)
HadAM3	3 m	All soil layers are active, e.g., contain roots	Saturation water content	Not defined	Function of soil type	Four layers with soil depth of 0.1, 0.25, 0.65, and 2 m
NCEP GFS	2 m	All soil layers are active, e.g., contain roots	Saturation water content	Function of soil type (Zobler 1986)	Function of soil type (Zobler 1986)	Two layers: 10- and 200-cm depth
NSIPP	Function of vegetation type	Function of vegetation type	Saturation water content	Function of vegetation type	Function of vegetation type	Three layers: surface, root zone, and deep recharge layers

for the given time of year and corresponding anomalies, subtracting the equation mean, and ignoring higher-order terms, the following (semi-implicit) equation for the autocorrelation of soil moisture between the time steps  $n$  and  $n + 1$  can be derived:

$$\begin{aligned} \rho &= \frac{\text{cov}(w_n, w_{n+1})}{\sigma_{w_n} \sigma_{w_{n+1}}} \\ &= \frac{\sigma_{w_n}}{\sigma_{w_{n+1}}} \left[ \left( \frac{2 - \frac{c\bar{R}_n}{C_s} - \frac{a\bar{P}_n}{C_s}}{2 + \frac{c\bar{R}_n}{C_s} + \frac{a\bar{P}_n}{C_s}} \right) + \frac{\text{cov}(w_n, F_n)}{\sigma_{w_n}^2} \right], \end{aligned} \quad (4)$$

where  $F$  is a combination of forcing terms and model parameters, depending linearly on  $P$  and  $R$ . For discussion purposes, we also present here the explicit form of Eq. (4), since it can be more easily interpreted:

$$\rho = \frac{\sigma_{w_n}}{\sigma_{w_{n+1}}} \left[ \left( 1 - \frac{c\bar{R}_n}{C_s} - \frac{a\bar{P}_n}{C_s} \right) + \frac{\text{cov}(w_n, F_n)}{\sigma_{w_n}^2} \right]. \quad (5)$$

Equation (4), and its explicit form (5), thus break down soil moisture memory into contributions from four separate terms:  $(\sigma_{w_n}/\sigma_{w_{n+1}})$ ,  $(c\bar{R}_n/C_s)$ ,  $(a\bar{P}_n/C_s)$ , and  $[\text{cov}(w_n, F_n)/\sigma_{w_n}^2]$ . The term  $(\sigma_{w_n}/\sigma_{w_{n+1}})$  represents the seasonality of soil moisture (changes in soil moisture variance from one month to the next), the terms  $(c\bar{R}_n/C_s)$  and  $(a\bar{P}_n/C_s)$  represent the sensitivity of evaporation and runoff on soil moisture content, and the term  $[\text{cov}(w_n, F_n)/\sigma_{w_n}^2]$  is a function of the covariance of soil moisture and subsequent forcing, thus reflecting both the memory of external forcing and land–atmosphere feedbacks.

From Eq. (5), soil moisture memory is seen to decrease with increasing values of  $(c\bar{R}_n/C_s)$  and  $(a\bar{P}_n/C_s)$ ; indeed, in cases of high values of these two terms, positive anomalies in soil moisture will be associated with subsequent positive anomalies of evaporation or runoff (with same forcing), which will in turn reduce the original soil moisture anomaly and thus induce a reduction of soil moisture memory for this given time period. Conversely, the term  $[\text{cov}(w_n, F_n)/\sigma_{w_n}^2]$  induces an increase in soil moisture memory, since it is associated with land–atmosphere feedbacks and/or memory in the forcing. Finally the term  $(\sigma_{w_n}/\sigma_{w_{n+1}})$  acts to increase or decrease the impact of the three other terms, thus either enhancing or damping their effects. In section 5, we will examine the magnitude of these four terms in the investigated AGCMs for (near) monthly time lags and show how they explain the geographical and inter-

model variations in simulated soil moisture memory. Variations of these terms with soil moisture regime and consequent impacts on soil moisture memory will be discussed in section 6.

As a final note, the linearizations underlying (2) and (3) necessarily imply simplifications in the analysis. Soil moisture has distinct upper and lower bounds, and the complex control of these bounds on memory are effectively captured here in a simple way by the evaporation and runoff sensitivity terms, which become very large as the lower or upper bound, respectively, is approached. A more complex framework—one that more explicitly treats these bounds and other nonlinearities and thresholds in the soil moisture problem—could be desirable for some regions, as results with stochastic–dynamical models suggest (e.g., Laio et al. 2001; Porporato and D’Odorico 2004). Nonetheless, the framework of (4) does allow its own complex elements of analysis. For example, it explicitly distinguishes several factors contributing to soil moisture memory, and because the linear regressions in (2) and (3) are performed independently at each grid point, it does not presuppose the same dependency of evapotranspiration and runoff on soil moisture at each location. Previous studies (KS01; Mahanama and Koster 2003) have demonstrated that (4) is generally a good approximation of soil moisture autocorrelation in a LSM or AGCM framework, despite the complexity of the problem.

### 3. Mean climate and biases of the AGCMs

In this section, we present the mean climatic and hydrological characteristics of the analyzed simulations as well as a brief evaluation of the precipitation and net surface radiation fields for the AGCMs’ mean. (A more detailed validation of individual model biases will be provided in section 5c). This examination will be useful for interpreting the results of the soil moisture memory analysis. Note that for all calculations involving evaporation in this study, we use a water-balance estimate of  $E$  [derived as  $P_{n,y} - Q_{n,y} - C_s(w_{n+1,y} - w_{n,y})$ ], as the evaporation outputted by some models did not always correspond to soil areas (e.g., due to lakes in the NSIPP model). Note as well that for all computations, the first 8 days of each simulation are disregarded in order to avoid spinup problems in the atmospheric part of the simulations (the spinup of soil moisture is not an issue given the design of the GLACE experiments). For the computation of the AGCMs’ average, the NCEP grid (highest resolution so as not to lose information; see Table 1) was chosen as the common grid and the values of the other AGCMs were interpolated to this common grid.

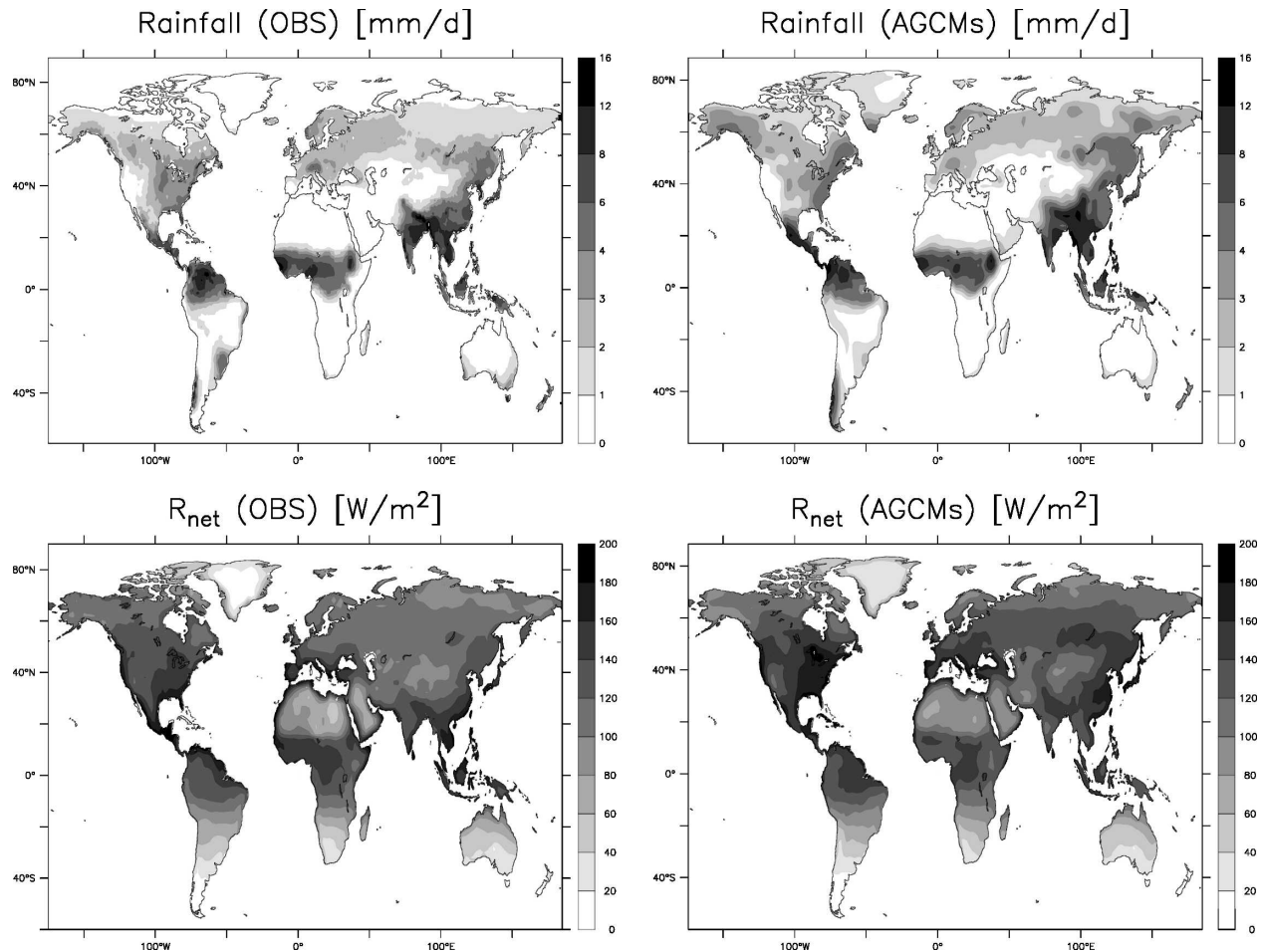


FIG. 1. (top left) Observed rainfall (GSWP forcing data; JJA) ( $\text{mm day}^{-1}$ ); (top right) AGCMs' average simulated rainfall ( $\text{mm day}^{-1}$ ); (bottom left) observed net radiation (ISLSCP SRB data; JJA) ( $\text{W m}^{-2}$ ); and (bottom right) AGCMs' average simulated net radiation ( $\text{W m}^{-2}$ ).

Figure 1 shows observed [June–August (JJA)] precipitation and net surface radiation (left) and the corresponding simulated fields averaged over the eight analyzed AGCMs (right), for the whole analysis period. The radiation observations correspond to a 7-yr (1984–90) climatology from the Surface Radiation Budget (SRB) dataset; the precipitation observations are taken from the Global Soil Wetness Project (GSWP) forcing data (climatology for 1983–95) and thus reflect a combination of Global Precipitation Climatology Centre (GPCC; Rudolf et al. 1994) and Global Precipitation Climatology Project (GPCP; Huffman et al. 1997) estimates (see Zhao and Dirmeyer 2003 for details). Note that the AGCMs' precipitation fields are generated for a single set of prescribed SSTs, while the observations cover many years and thus reflect many different sets of SSTs. Thus, some portion of the biases shown may simply reflect SST-induced rainfall variations and not necessarily model error. This is particularly true in the

Tropics, where SSTs have a significant impact on inter-annual rainfall variations.

Precipitation is on average well simulated in the models, with a proper placement of high- (Southeast Asia, equatorial Africa, northern tip of South America) and low- (deserts) precipitation areas. Some bias is found in the northern high latitudes (Alaska, Siberia), where the AGCMs tend on average to overestimate precipitation. Net surface radiation is also relatively well captured, but there are clear positive biases, particularly in the eastern United States, as well as across Eurasia. Thus, in the mean, precipitation and radiation appear to be fairly well simulated in the models. A discussion of individual model biases will be provided in section 5c.

Figure 2 displays further average climatic and hydrological characteristics of the AGCMs over the analysis period. As expected, the mean AGCMs' soil moisture in the midlatitudes and the Tropics is generally high in

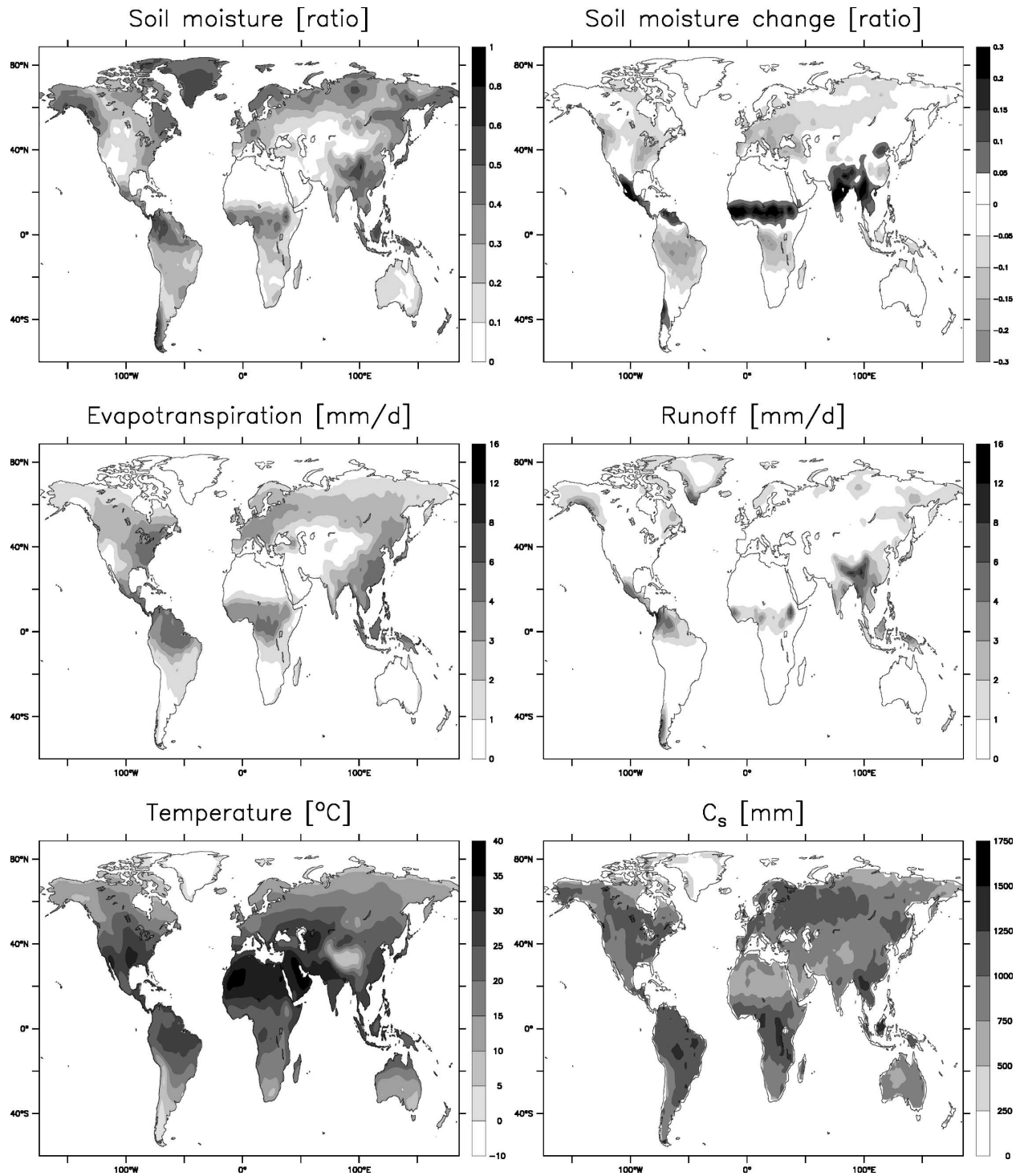


FIG. 2. (top left) AGCMs' average simulated soil moisture; (top right) AGCMs' average simulated monthly changes in soil moisture; (middle left) AGCMs' average simulated evaporation ( $\text{mm day}^{-1}$ ); (middle right) AGCMs' average simulated runoff ( $\text{mm day}^{-1}$ ); (bottom left) AGCMs' average simulated air temperature ( $^{\circ}\text{C}$ ); and (bottom right) AGCMs' average water-holding capacity  $C_s$ .

the regions of high precipitation. The relatively high values found in the northern high latitudes are likely linked with snowmelt. Regions experiencing large increases in soil moisture over the 3-month simulation period are found in the Tropics and monsoon regions of Asia, Africa, and North America, whereas those experiencing large reductions in soil moisture are generally in the midlatitudes. Evaporation is generally high in regions of high soil moisture content and warm air temperature, and also appears correlated with water-holding capacity. Note that evaporation is high even in regions experiencing an increase in soil moisture over the simulated three-month period (e.g., Southeast Asia, equatorial Africa). Runoff, for its part, is high mostly in Southeast Asia, particularly in the Ganges region.

#### 4. Overall soil moisture memory characteristics of the AGCMs

Soil moisture autocorrelations are computed for each AGCM (from the 16 ensemble simulations) for three 27-day periods delimited at the following time steps: 9, 36, 63, and 90 (the GLACE data being available as daily output). They are then averaged over these three periods. Again, the first 8 days of each simulation are disregarded. The autocorrelations are computed in two ways: (a) directly from the models' soil moisture values on the four indicated days, and (b) using (4). In this section, we will first analyze the overall soil moisture memory characteristics of the AGCMs [point (a)] and present a brief validation of these results with soil moisture observations. A more detailed analysis using the KS01 framework [point (b)] follows in section 5.

##### a. Geographical variations in soil moisture memory

The 27-day autocorrelation fields  $\rho_{27}$  computed directly from the soil moisture fields for each model [point (a) above] are averaged to produce the multimodel estimate of memory shown in Fig. 3 (top). Given the lack of ground observations of soil moisture and the potential for biases associated with the analysis of any individual model alone, this represents to a large extent the "best" present global estimate of this quantity, as simulated in current AGCMs. On average, the models are characterized by high soil moisture memory in mid-latitude regions and by low soil moisture memory in tropical regions. Interestingly, almost all regions of low soil moisture memory are also characterized by high precipitation (Fig. 1) and high mean soil moisture (Fig. 2), and are therefore typically humid regions. Note the asymmetric distribution of low soil moisture memory

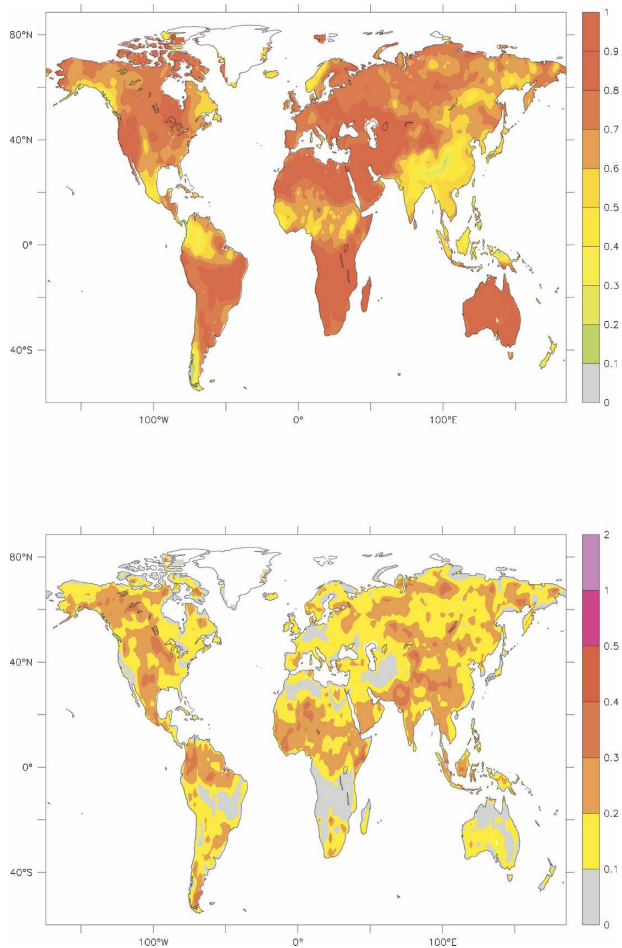


FIG. 3. (top) AGCMs' average values of  $\rho_{27}$ ; (bottom) std dev of  $\rho_{27}$  among AGCMs.

regions around the equator, due to the 3-month period under consideration (boreal summer). Regions of low soil moisture memory extend far to the north in East Asia, linked with the monsoon climate of this region. Similarly, the North American monsoon system (NAMS) region (Mexico, southern United States) displays lower soil moisture memory than the rest of North America.

An indication of the intermodel differences in soil moisture memory (and thus of the uncertainty of the multimodel average presented in the top plot of Fig. 3) is the standard deviation of  $\rho_{27}$  among the models (Fig. 3, bottom). Strikingly, the largest spread appears in regions displaying low soil moisture memory. This suggests that there is less agreement on soil moisture memory characteristics in humid climates among the models. A more detailed discussion of intermodel differences in soil moisture memory will be provided in section 5c.

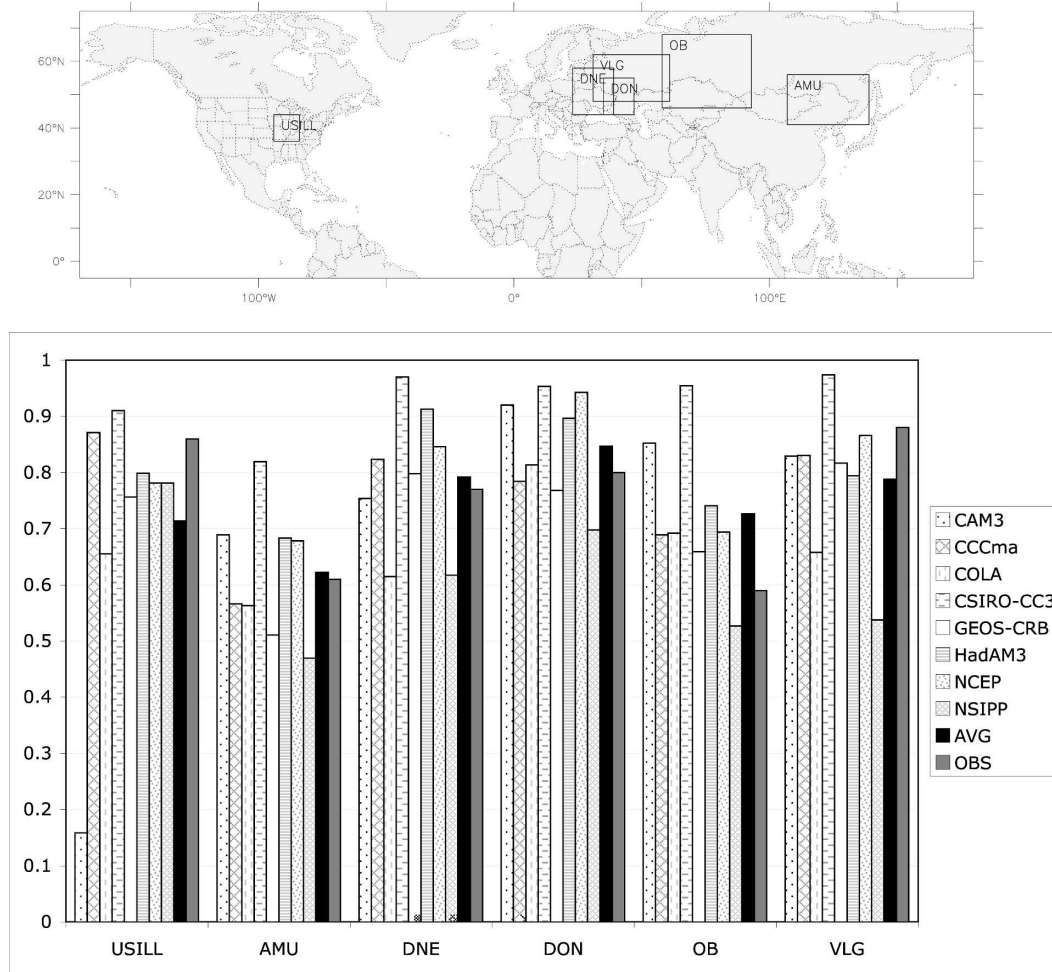


FIG. 4. (top) Regional boxes used for comparison with soil moisture observations: Illinois (USILL), Dnepr (DNE), Don, Volga (VLG), Ob, and Amur (AMU); (bottom) histograms of soil moisture autocorrelation for all AGCMs ( $\rho_{27}$ ; light gray bars), the AGCMs' average (black bar), and the observations ( $\rho_{\text{monthly}}$ ; dark gray bar) in the regional boxes defined above.

### b. Comparisons with soil moisture observations

As mentioned earlier, there are only few ground observations of soil moisture available for the analysis of regional soil moisture memory characteristics. It is nonetheless interesting to evaluate to which extent the multimodel estimate of Fig. 3 (top) agrees with the available observations. We compare here regional or basinwide averages of soil moisture observations with the AGCMs' results. The observations are taken from Hollinger and Isard (1994) for Illinois and from the Global Soil Moisture Data Bank (Robock et al. 2000) for the Amur, Dnepr, Don, Ob, and Volga River basins. The regional and basinwide average values were compiled for use in previous studies (Seneviratne et al. 2004; Hirschi et al. 2006). Note that we compare here values for 27-day periods (simulations) and 30-/31-day

periods (observations). One should therefore expect the simulation values to be slightly biased high compared to the monthly observations. Moreover, the observations are taken for a fixed soil depth (down to 1 m for the measurements in the former Soviet Union, and down to 2 m in Illinois), while we consider the total column of available soil water (as defined in section 2) in the AGCMs.

The top part of Fig. 4 displays the boxes used for the analysis, while the bottom part displays histograms of  $\rho_{27}$  for each AGCM (light gray bars), together with the multimodel AGCM estimate (black bar) and the observed monthly autocorrelation value (dark gray bar). In general, the models are close to the observations and are able to distinguish between regions of low or high soil moisture memory. Note that the models' average value agrees generally well with the observations, par-

ticularly in the Amur, Dnepr, Don, and Volga River basins.

This comparison also pinpoints a few outliers among the analyzed AGCMs. The CAM3 AGCM clearly underestimates soil moisture memory in Illinois. In general the COLA and NSIPP AGCMs tend to have low soil moisture memory in many regions, likely due to their comparatively low values of  $C_s$  (see section 5d). The CSIRO-CC3 AGCM, which has relatively high values of  $C_s$ , tends for its part to have a positive bias in soil moisture memory. These intermodel differences and the relevance of model biases for the simulated soil moisture memory will be discussed in more detail in sections 5c and 5d, respectively.

Despite the presence of outliers, the comparisons with the available observations are encouraging, in particular given the scale discrepancy between the AGCM simulations and the point-scale observations used for the basin averages. These results suggest that in the mean the analyzed AGCMs correctly capture the processes controlling soil moisture memory in the considered regions.

## 5. Analysis of soil moisture memory with KS01 autocorrelation equation

In this section, we investigate the soil moisture memory characteristics of the simulations using the KS01 soil moisture memory Eq. (4). Again, we analyze soil moisture memory characteristics averaged over three 27-day periods (see section 4). Hence, the 27-day average fluxes and the daily soil moistures at the beginning and end of each 27-day period were used to compute the terms in Eq. (4). We will first compare the equation estimates of soil moisture memory with the actual soil moisture memory of the models, in order to validate the chosen framework. Then, the AGCMs' mean soil moisture characteristics as well as intermodel differences and geographical variations in soil moisture memory will be investigated.

### a. Agreement of autocorrelation equation with simulated soil moisture memory

Figure 5 displays maps of the AGCMs' 27-day-lagged soil moisture autocorrelation, of the corresponding values of soil moisture autocorrelation computed with Eq. (4), and of their difference. The white areas on the plots correspond to regions covered with snow or permanent ice, or to grid points characterized with soil moisture variance of zero due to peculiarities of the individual models. The limited sample size (48 points) used in the calculation of autocorrelations in this paper

necessarily leads to some error in the autocorrelation estimates [in addition to the errors associated with the approach itself, and in particular the linearization assumptions made in (2) and (3)]. Monte Carlo analysis shows that the root-mean-square error (RMSE) of an autocorrelation estimate based on a sample size of 48 ranges from 0.15 for low autocorrelations (0.1–0.2) to 0.13 for high autocorrelations (0.8–0.9). The areas shaded in gray in the plots correspond to errors of below 0.15.

For most regions and models, Eq. (4) represents a very good approximation of the AGCMs' soil moisture memory. The intermodel and intramodel variations in soil moisture memory are both clearly captured. There are only a few discrepancies, mostly in Southeast Asia (CCCma, CSIRO-CC3, and HadAM3) and in the northwestern part of South America (CCCma, CSIRO-CC3, GEOS-CRB, and HadAM3). The very good agreement between the AGCMs' simulated soil moisture memory and the autocorrelation values derived with Eq. (4) confirms previous results with the NSIPP AGCM and uncoupled land surface models (KS01; Mahanama and Koster 2003) showing that (4) is an appropriate framework for analyzing model and regional differences in simulated memory.

### b. Equation terms: Average across models

To assess the relative impact of the four terms of Eq. (4), Fig. 6 displays maps of  $(\sigma_{w_n}/\sigma_{w_{n+1}})$ ,  $[\text{cov}(w_n, F_n)/\sigma_{w_n}^2]$ ,  $(c\bar{R}_n/C_s)$ , and  $(a\bar{P}_n/C_s)$ , averaged across the models. For the analysis and intercomparison of these terms, it is helpful to keep in mind the explicit form of (4), that is, (5). In the top two plots, values contributing to an increase in soil moisture memory are shaded in warm colors and values contributing to a decrease in soil moisture memory are shaded in cold colors; the opposite is true for the two bottom plots. One should note that due to all the nonlinearities involved, these AGCMs' average equation terms provide only a rough, flawed estimate of the AGCMs' average autocorrelations when recombined in (4) (not shown). Nonetheless, the averages of the terms are still of interest, since they provide a first-order look at what controls the global distribution of soil moisture memory.

A comparison of Fig. 6 (top) with Fig. 3 reveals that, except for the NAMS region, areas of low soil moisture memory are generally associated with high values of  $(a\bar{P}_n/C_s)$ . This is consistent with the aforementioned fact that low soil moisture memory values are generally found in humid areas (equatorial and tropical regions, monsoon regions), where one expects the runoff's sensitivity on soil moisture to be the highest. Note, nonetheless, that in these areas the evaporation sensitivity

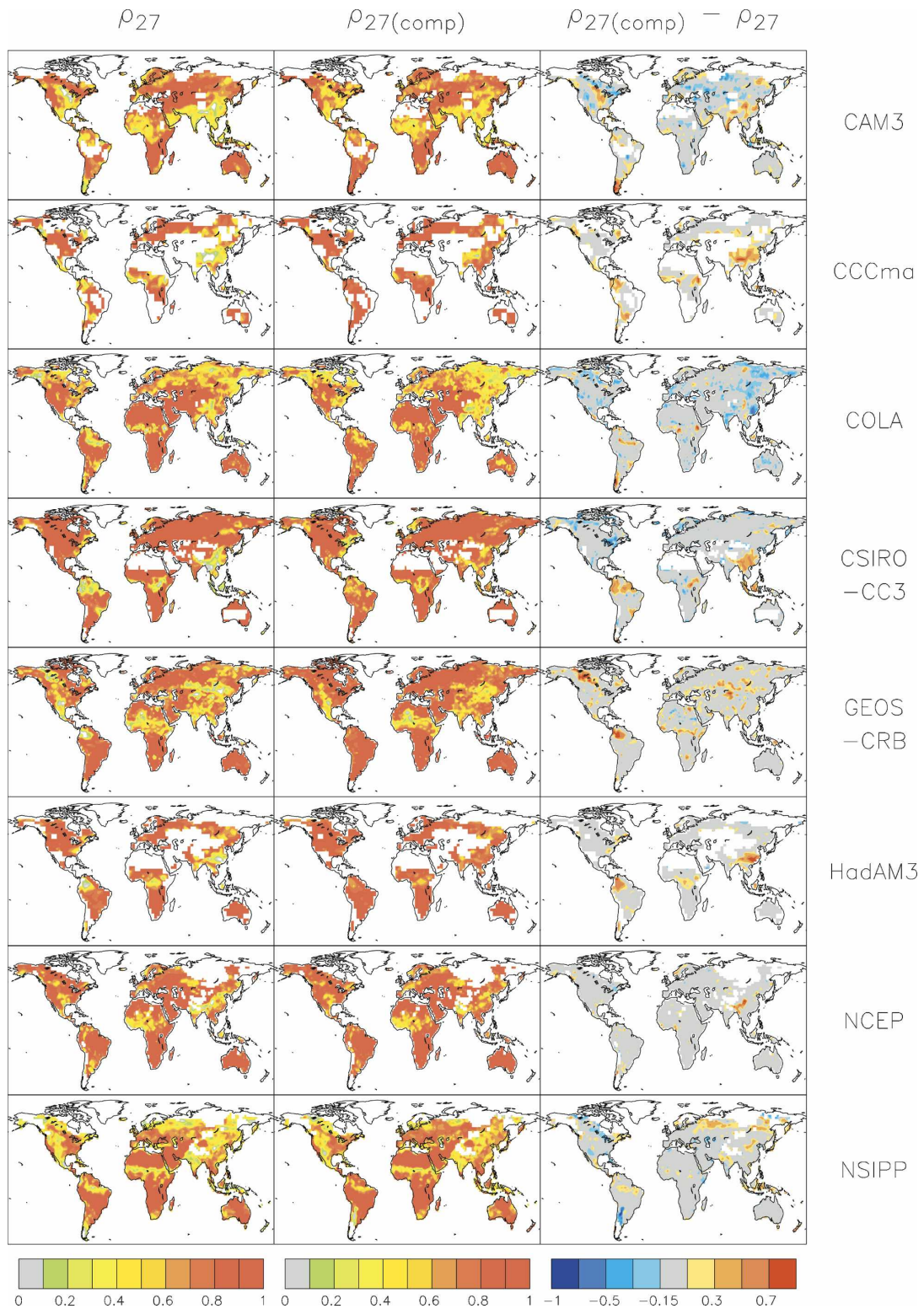


FIG. 5. (left) Maps of simulated 27-day-lagged autocorrelation of total profile soil moisture  $\rho_{27}$  in the eight AGCMs. (middle) Corresponding maps of  $\rho_{27}(\text{comp})$  as estimated with Eq. (4). (right) Differences, i.e., estimated autocorrelations minus simulated autocorrelations.

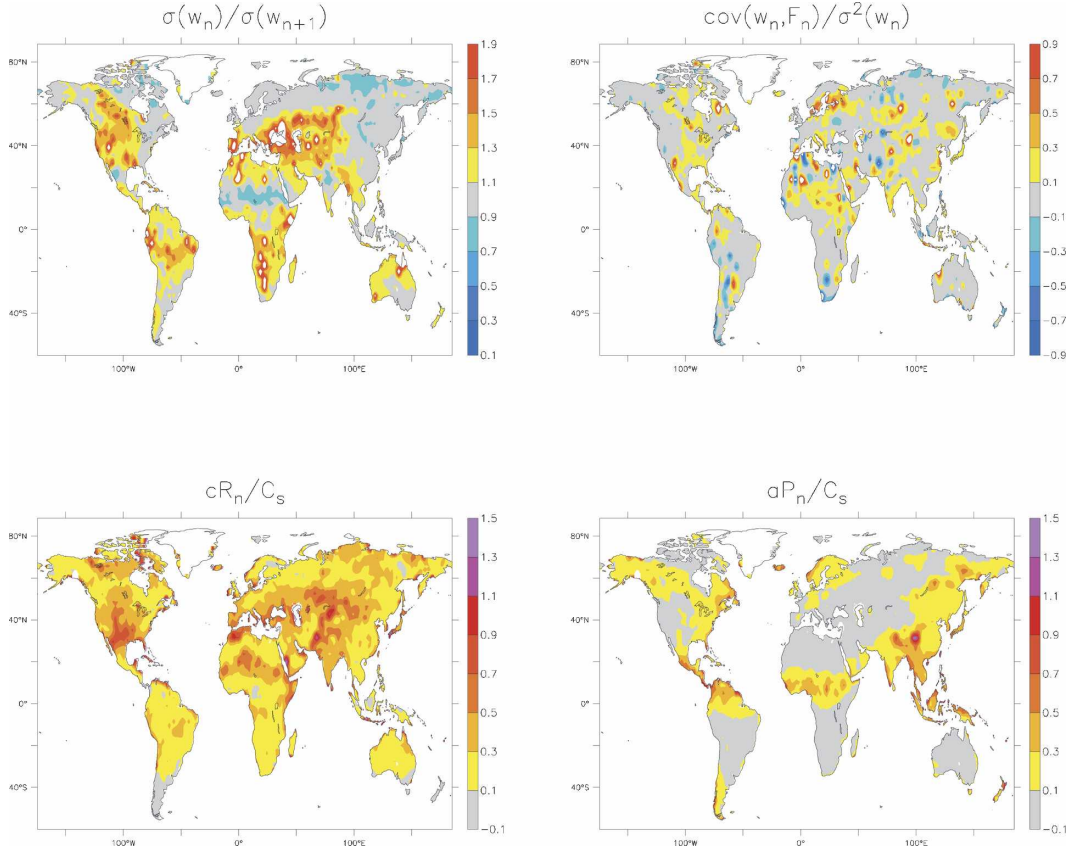


FIG. 6. Maps of mean AGCMs' values of (top left)  $(\sigma_{w_n}/\sigma_{w_{n+1}})$ ; (top right)  $[\text{cov}(w_n, F_n)/\sigma_{w_n}^2]$ ; (bottom left)  $(c\bar{R}_n/C_s)$ ; and (bottom right)  $(a\bar{P}_n/C_s)$ .

term  $(c\bar{R}_n/C_s)$  can often be almost as large as  $(a\bar{P}_n/C_s)$  and therefore also contributes to lowering soil moisture memory. Interestingly, areas characterized by high values of  $(c\bar{R}_n/C_s)$  are generally not systematically characterized by low soil moisture memory, which may seem surprising given the magnitude of this term across the globe in Fig. 6. This is generally due to a compensation by the seasonality term (western part of northern United States and Canada, southern Europe, and central Asia). Explanations for this behavior will be discussed in section 6b. Reductions of soil moisture memory due to  $(c\bar{R}_n/C_s)$  are nonetheless clear in south-central North America (more or less coincident with the NAMS region), in the Sahel, and in India. The seasonality term  $(\sigma_{w_n}/\sigma_{w_{n+1}})$  reduces memory only in the Sahel region, western Mexico, central India, and Siberia. It is high during boreal summer over Northern Hemisphere areas with Mediterranean climates (winter wet, summer dry) and in some cases semiarid climate (central Asia), and in Southern Hemisphere monsoon regions that are in their dry season. Finally, this analysis shows that the values of the  $[\text{cov}(w_n, F_n)/\sigma_{w_n}^2]$  term for the AGCMs' mean are generally small (which might be

due in part to the nonaccounting of interannual variations of SST in the experimental design; see section 2a) and that the geographical distribution of this term is similar to that of the  $\Omega$  factor representative of the coupling strength of the models (Koster et al. 2004a, 2006; see also section 7); this latter point highlights the importance of land–atmosphere feedbacks as opposed to externally induced memory in the forcing for this term. Note that, because of its link with evapotranspiration (e.g., Guo et al. 2006), this term often impacts a slight compensation of the evaporation sensitivity term  $(c\bar{R}_n/C_s)$  in regions of high land–atmosphere coupling.

### c. Equation terms: Intermodel differences

Figure 7 displays maps of the standard deviation among the AGCMs of the terms  $(\sigma_{w_n}/\sigma_{w_{n+1}})$ ,  $[\text{cov}(w_n, F_n)/\sigma_{w_n}^2]$ ,  $(c\bar{R}_n/C_s)$ , and  $(a\bar{P}_n/C_s)$ . These maps can be seen as the uncertainty of the multimodel estimates displayed in Fig. 6.

The standard deviation of the equation terms is in general highest for higher values of the terms. Note that high deviations in the equation terms can sometimes be caused by only one anomalous AGCM. This is for in-

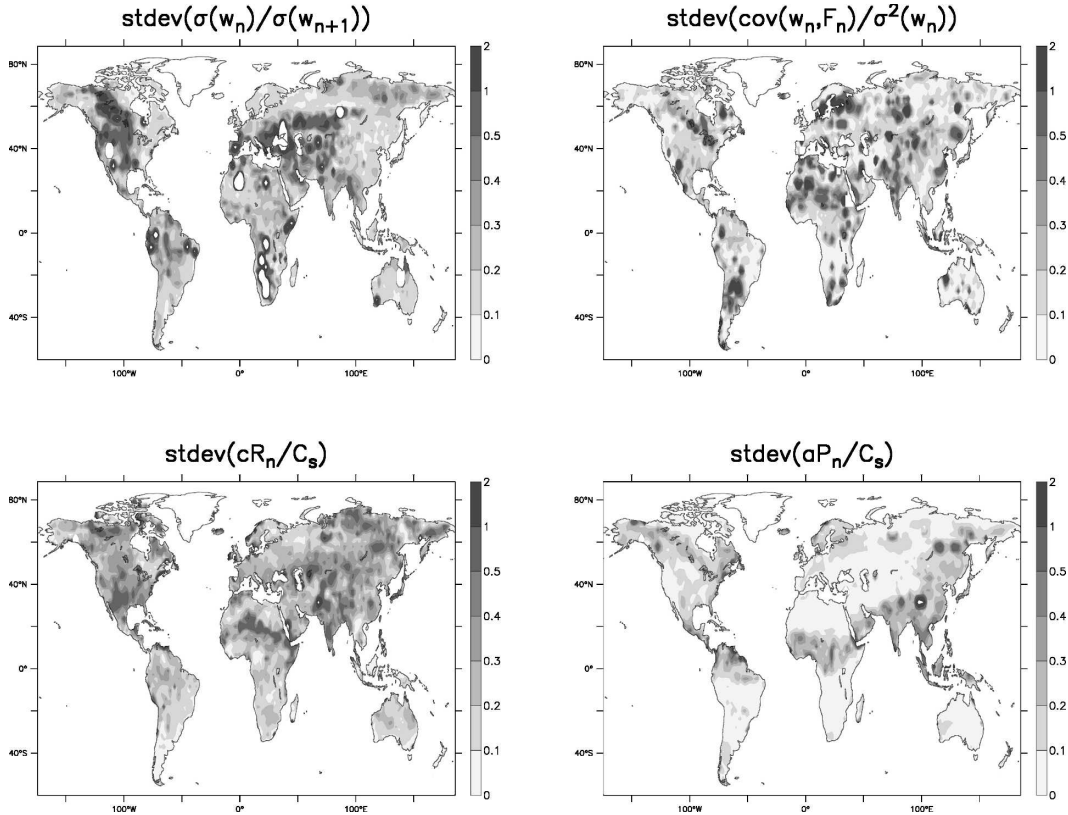


FIG. 7. Maps of standard deviation among the AGCMs of (top left)  $(\sigma_{w_n}/\sigma_{w_{n+1}})$ ; (top right)  $[\text{cov}(w_n, F_n)/\sigma_{w_n}^2]$ ; (bottom left)  $(\overline{cR_n}/C_s)$ ; and (bottom right)  $(\overline{aP_n}/C_s)$ .

stance the case for  $(\sigma_{w_n}/\sigma_{w_{n+1}})$ : The high values and high standard deviation of this term in North America and central Asia are mostly caused by very high values of this term for the GEOS-CRB AGCM (not shown). Also, most of the high values in the standard deviation of the  $[\text{cov}(w_n, F_n)/\sigma_{w_n}^2]$  term are due to very high values in the CAM3 model, which reflect low variance of the soil wetness term rather than land-atmosphere feedbacks (not shown). In the case of the  $(\overline{cR_n}/C_s)$  and  $(\overline{aP_n}/C_s)$  terms, high standard deviations generally reflect a discrepancy between a larger number of models (not shown).

To investigate such intermodel differences in more detail, we now focus on the analysis of five selected regions with location displayed in Fig. 8: south-central North America (SCNA), equatorial Africa (EQAF), northern India (NIND), Southeast Asia (SEA), and the Volga River basin (VLG). These regions were chosen in order to sample a wide range of soil moisture memory characteristics. Figures 9 and 10 display for each AGCM and the AGCMs' mean the average values in these five regions of  $\rho_{27}$ ,  $\rho_{27(\text{comp})}$ ,  $(\sigma_{w_n}/\sigma_{w_{n+1}})$ ,  $A_n$  [see Eq. (4)],  $[\text{cov}(w_n, F_n)/\sigma_{w_n}^2]$ ,  $(\overline{cR_n}/C_s)$ ,  $(\overline{aP_n}/C_s)$ ,  $(C_s/1000)$  (water-holding capacity in meters), and the  $r^2$  values of the

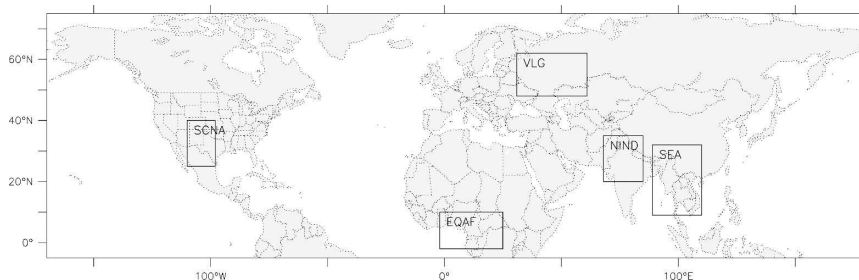


FIG. 8. Boxes used for the regional analysis: south-central North America (SCNA), equatorial Africa (EQAF), northern India (NIND), Southeast Asia (SEA), and Volga (VLG).

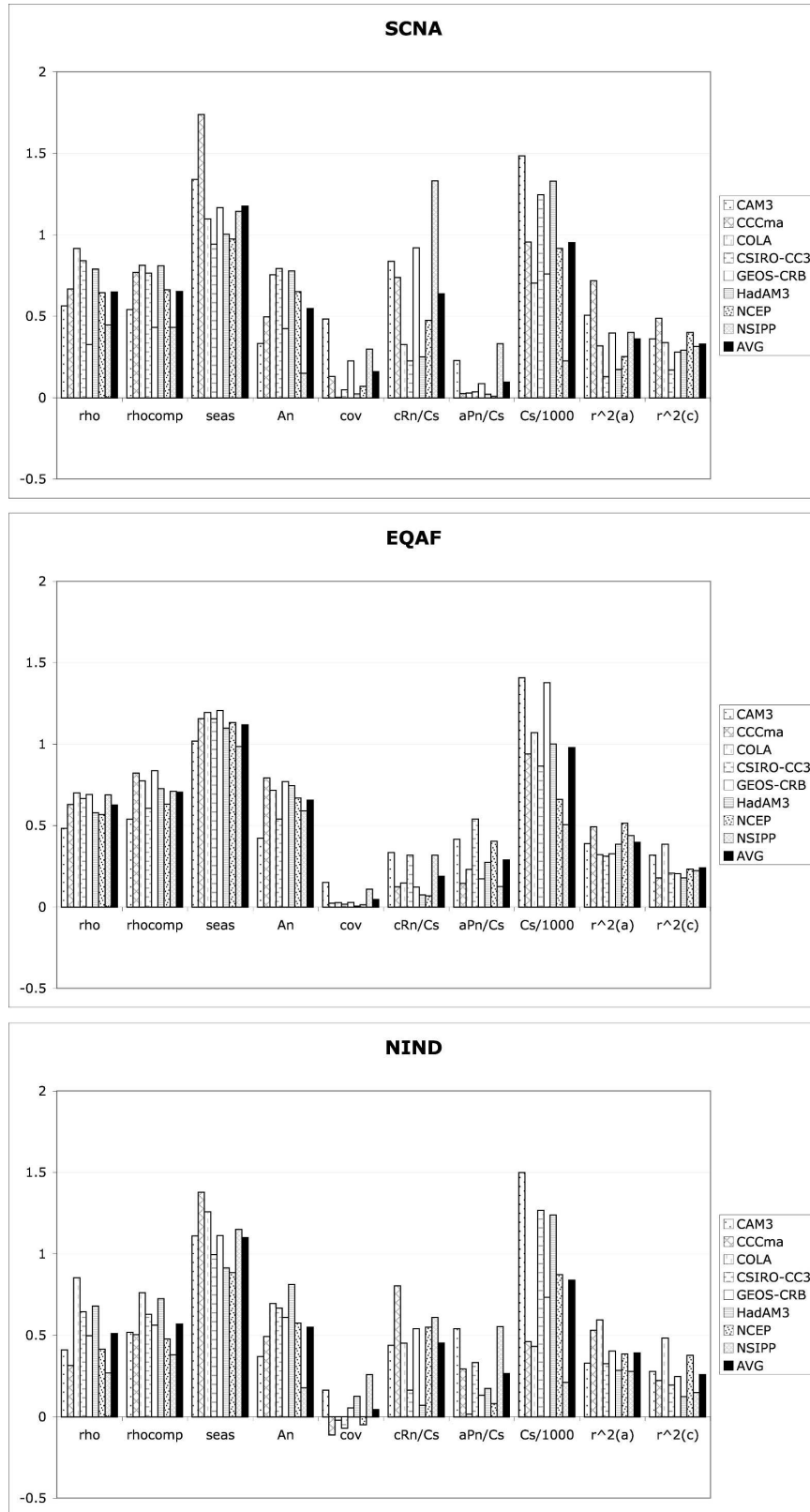


FIG. 9. Regional analyses in the boxes defined in Fig. 8 (SCNA, EQAF, and NIND).

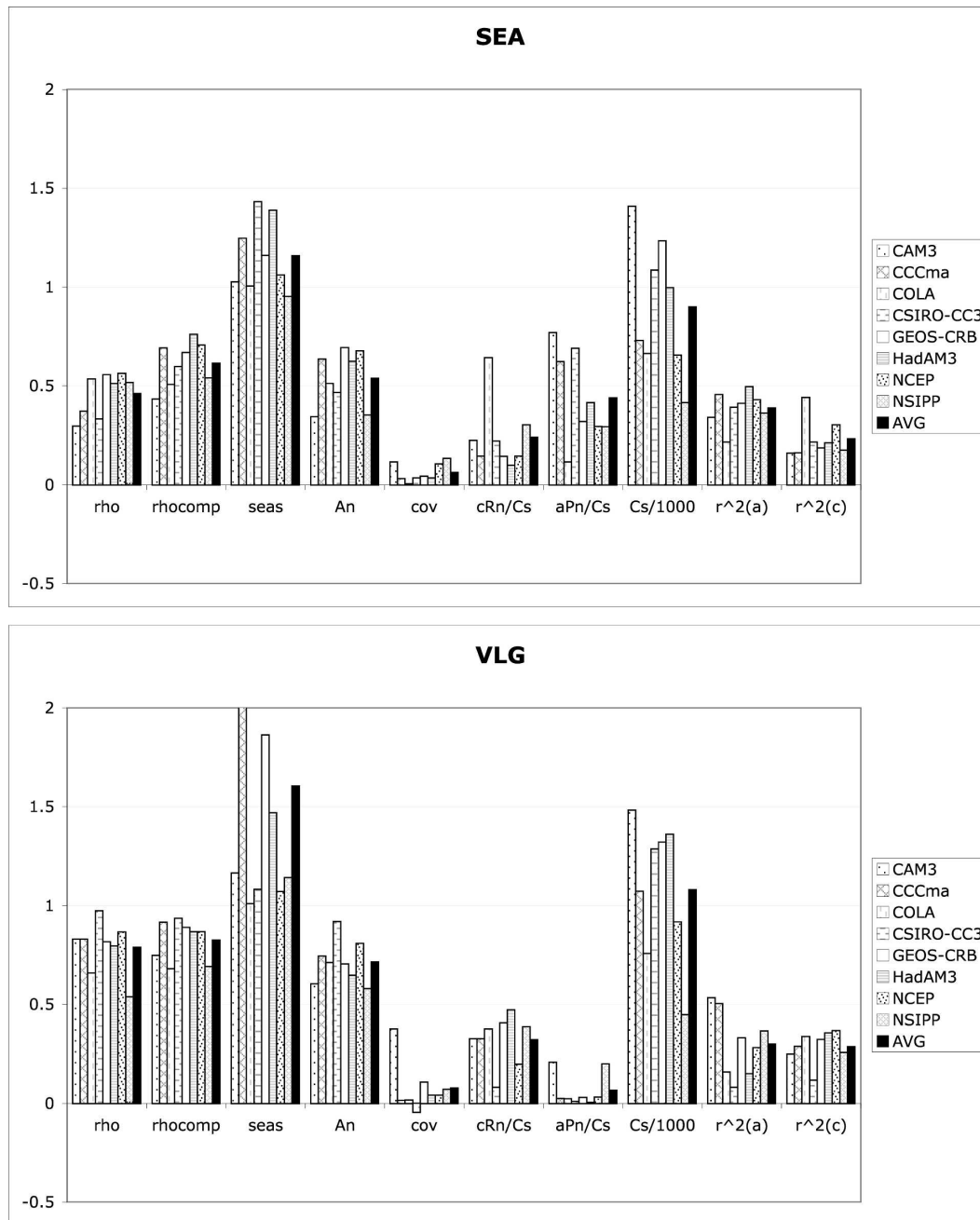


FIG. 10. Regional analyses in the boxes defined in Fig. 8 (SEA and VLG).

linear regressions performed in order to determine  $a$  and  $c$  [Eqs. (2) and (3)].

For all five regions,  $\rho_{27(\text{comp})}$  is a good estimate of  $\rho_{27}$ . Despite slight overestimations in the SEA and NIND regions,  $\rho_{27(\text{comp})}$  is seen to capture both intermodel and regional differences in  $\rho_{27}$ , as previously discussed in section 5a. Note that this is the case despite the fact that the  $r^2$  values of the linear regressions are not extremely high in most regions. Concerning the  $r^2$  values, Monte

Carlo simulations show that estimates of  $a$  and  $c$  (slopes) with an  $r^2$  exceeding 0.08 are significantly different from zero at the 95% level (not shown). This significance test is satisfied for both  $a$  and  $c$  in all five regions (and indeed across most of the globe; not shown).

Interestingly, intermodel differences in soil moisture memory can be as large as regional differences in this quantity. Water-holding capacity is seen to be an im-

portant factor for such intermodel differences, in particular for the NSIPP AGCM, which has low values of  $C_s$  and corresponding low values of soil moisture memory in many of the considered regions. Note that the effect of  $C_s$  on intermodel variations in soil moisture memory is particularly clear in the SCNA, NIND, and VLG regions.

As previously analyzed for the AGCMs' mean behavior, the terms  $(c\bar{R}_n/C_s)$  and  $(a\bar{P}_n/C_s)$  are the most important of the four terms of Eq. (4) in controlling soil moisture memory for the various models and regions. The  $A_n$  term, which approximately corresponds to  $[1 - (c\bar{R}_n/C_s) - (a\bar{P}_n/C_s)]$  [see (5)] is seen indeed to be closely correlated with the  $\rho_{27}$  and  $\rho_{27(\text{comp})}$  values. The term  $[\text{cov}(w_n, F_n)/\sigma_{w_n}^2]$  is generally small (possibly due in part to the nonaccounting of interannual SST variations; see section 2a), while the term  $(\sigma_{w_n}/\sigma_{w_{n+1}})$  is generally close to 1. Thus, these two terms have only a small impact on overall soil moisture memory.

#### d. Importance of AGCMs' biases for simulated soil moisture memory

An important question is the extent to which the simulated soil moisture memory of the AGCMs is distorted by model biases (e.g., Mahanama and Koster 2005). Here we focus on biases in atmospheric forcing (precipitation, radiation), as well as on water-holding capacity (for which no globally complete observations exist). The AGCMs' biases in atmospheric forcing are displayed in the left and middle columns of Fig. 11, and the water-holding capacity of the AGCMs is displayed in the right column of Fig. 11. The observational datasets described in section 3 are used for the assessment of the biases in atmospheric forcing.

As for the AGCMs' mean (section 3), precipitation is generally well represented in the individual models. One should note, however, that the GEOS-CRB AGCM presents a negative precipitation bias in North America, and that various models display positive precipitation biases in Southeast Asia (CCCma, COLA, CSIRO-CC3, GEOS-CRB, and NCEP). Biases in net surface radiation are significant, particularly for certain models: The COLA AGCM exhibits a high positive bias globally, while the GEOS-CRB AGCM has a large positive bias in Eurasia and in the eastern part of North America. At least in the case of the COLA AGCM, this radiation bias appears to be possibly linked with an underestimation of soil moisture memory (Fig. 5).

Water-holding capacity is highly variable among the AGCMs. For the same regions, differences can be as large as 1000 mm for some pairs of models. This is of course of major relevance for simulated soil moisture memory, as previously seen for selected regions (Figs. 9

and 10). Note that for the COLA and NSIPP AGCMs the distribution of  $\rho_{27}$  across the globe (Fig. 5) is highly correlated with variations in water-holding capacity. The importance of water-holding capacity can be easily understood if one considers Eqs. (4) and (5) and the impact of  $C_s$  on the terms  $(c\bar{R}_n/C_s)$  and  $(a\bar{P}_n/C_s)$ . A comparison of the original soil moisture autocorrelation values with estimates derived using (4) with observed precipitation and radiation fields as well as the AGCMs' mean water-holding capacity for each model shows that, for the set of models analyzed here, intermodel differences in  $C_s$  contribute more to intermodel differences in memory than do intermodel differences in forcing biases or land surface sensitivity (not shown). This is particularly true for the COLA and NSIPP AGCMs (see above).

## 6. Dependence of soil moisture memory on climate regime

In this section, we address in more detail the dependency of the simulated soil moisture memory on the regional climate regime as characterized by the average soil moisture content.

### a. Simulated and computed soil moisture memory

Figure 12 displays plots of  $\rho_{27}$  and  $\rho_{27(\text{comp})}$  as functions of soil wetness for each AGCM. (A simple binning procedure produced the curve shown for each model.) As expected, a sharp decrease in soil moisture memory is seen at high soil wetness values. Similar though more muted behavior is also seen for the soil moisture memory estimates derived with (4), as the right panel demonstrates. Interestingly, more than half of the models (CCCma, CSIRO, GEOS-CRB, HadAM3, and NCEP) exhibit a small decrease in soil moisture memory at low soil wetness, in addition to the decrease at high soil wetness. This thus results in a bell-shaped relationship between soil moisture memory and soil moisture content, with highest soil moisture memory values at intermediate soil wetness.

Note that the sharp decrease in  $\rho_{27}$  with increasing soil moisture, as well as the anomalous behavior of the CAM3 AGCM, explains the high variability in  $\rho_{27}$  found in humid regions, as identified in Fig. 3 (bottom). One should remark, however, that there are fewer grid points at high soil moisture than at low and intermediate soil moisture, which is responsible for some of the erratic behaviors in the tails; this is particularly relevant for the models with low resolution (see Table 1), as well as for CAM3, which is characterized by dry conditions over most of the globe. Given the parameterization specificities of CAM3, the soil wetness index used here

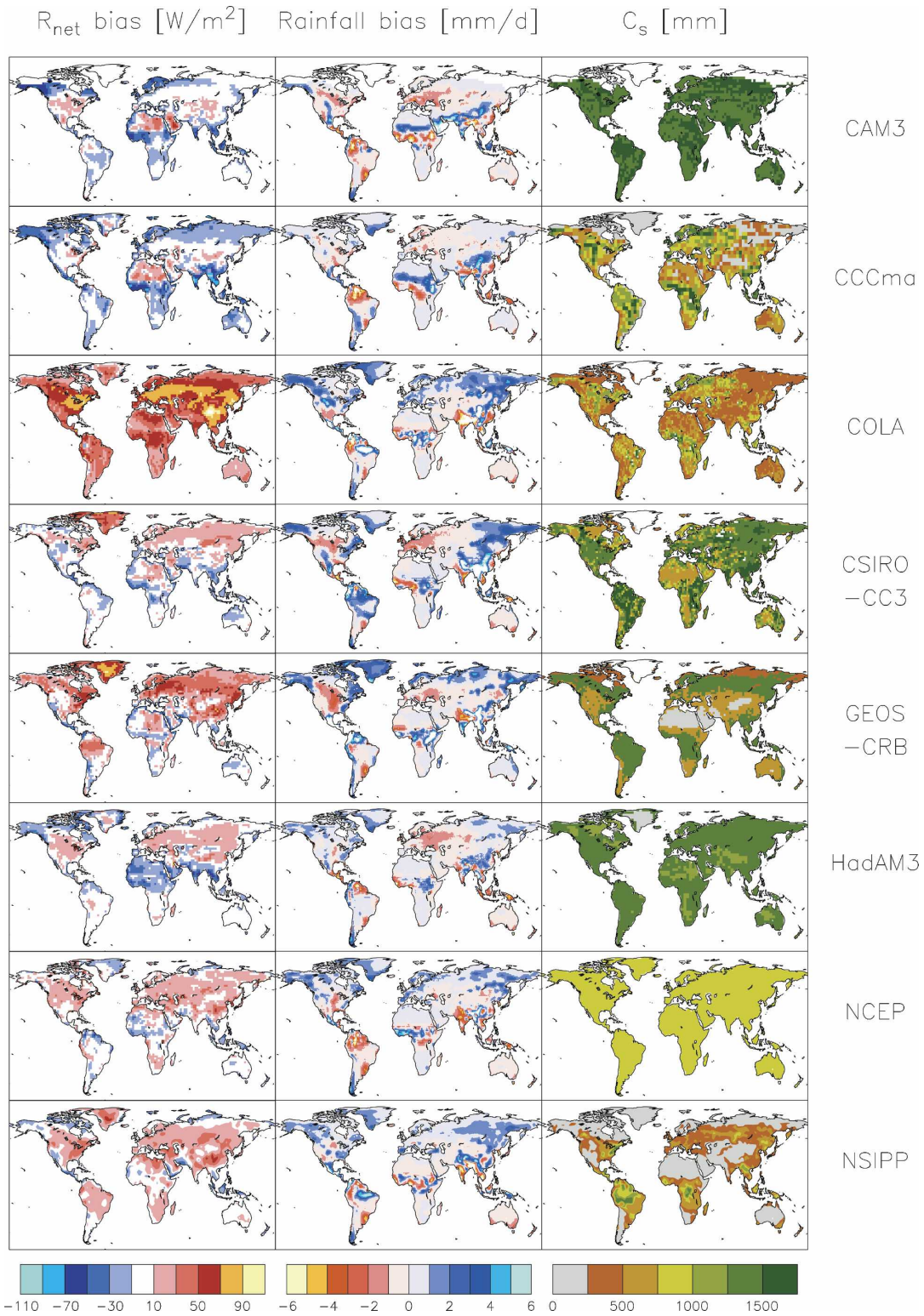


FIG. 11. (left) Biases in net surface radiation, (middle) biases in precipitation, and (right) water-holding capacity of the AGCMs ( $C_s$ ).

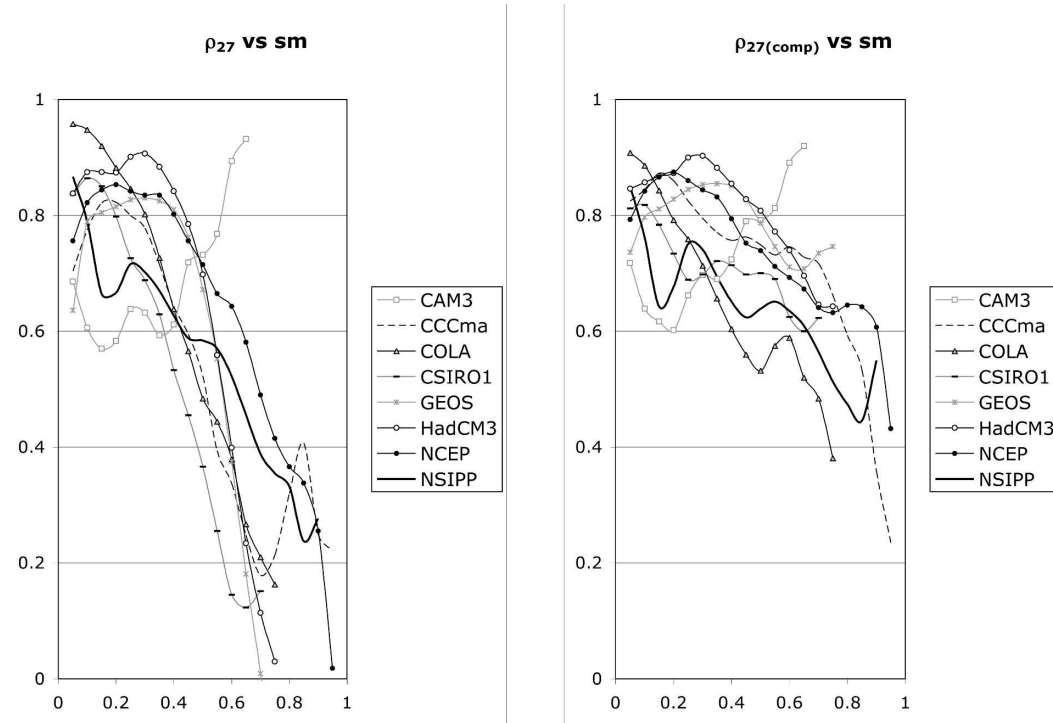


FIG. 12. Distribution of  $\rho_{27}$  and  $\rho_{27(comp)}$  as functions of soil moisture (computed as bins for given soil moisture ranges).

(section 2a) might not be the best estimate of prevailing soil moisture conditions for this model. A better estimate might likely be the “BTRAN” ( $\beta_t$ ) parameter, which ranges from one when the soil is wet to near zero when the soil is dry and depends on the root distribution of the plant functional type and the soil water potential of each soil layer (Oleson et al. 2004). A recomputation of the soil moisture memory values for CAM3 using the  $\beta_t$  parameter yields qualitatively similar results as the ones found for the other AGCMs (not shown).

#### b. Equation terms

Figure 13 displays the dependency of the equation terms ( $c\bar{R}_n/C_s$ ), ( $a\bar{P}_n/C_s$ ), ( $\sigma_{w_n}/\sigma_{w_{n+1}}$ ), and [ $\text{cov}(w_n, F_n)/\sigma_{w_n}^2$ ] on soil moisture. The most striking features of these plots are the exponential increase of ( $c\bar{R}_n/C_s$ ) at low soil moisture values and the exponential increase of ( $a\bar{P}_n/C_s$ ) at high soil moisture values. Thus, considering Eqs. (4) and (5), one can conclude that the decrease of soil moisture memory in humid regions can be linked with increases in the runoff sensitivity term ( $a\bar{P}_n/C_s$ ), while the decrease of soil moisture memory at low soil wetness for the five AGCMs identified above is linked with increases in the evaporation sensitivity term ( $c\bar{R}_n/C_s$ ). The remaining three AGCMs (CAM3, COLA, and

NSIPP) present somewhat different characteristics. As previously mentioned, the CAM3 AGCM’s behavior is presumably affected by the use of soil wetness instead of BTRAN for this analysis. The COLA and NSIPP AGCMs, while similar to the other five models at high soil moisture, differ from the others at low soil moisture, and also present a different dependency of ( $c\bar{R}_n/C_s$ ) on soil moisture. This might be due in part to their relatively low values of  $C_s$ , or (in the case of COLA) to a bias in radiation forcing (see section 5d).

With regards to ( $\sigma_{w_n}/\sigma_{w_{n+1}}$ ) and [ $\text{cov}(w_n, F_n)/\sigma_{w_n}^2$ ], though these terms were generally found to be less important than ( $a\bar{P}_n/C_s$ ) and ( $c\bar{R}_n/C_s$ ) in defining the geographical distribution of soil moisture memory, Fig. 13 shows that they can be important for some soil moisture regimes and models. One particularly striking aspect is the behavior of the seasonality term ( $\sigma_{w_n}/\sigma_{w_{n+1}}$ ), which in general increases at low and high soil moisture values and thus impacts a partial compensation of the evaporation and runoff sensitivity terms [see Eq. (5)]. This effect was also identified—mostly for the evaporation sensitivity term—in the analysis of the average model values of the equation terms in section 5b. Therefore, the seasonality term is not proportional to soil moisture memory, despite being a multiplying factor in (4) and (5); instead, its main impact appears to be a compen-

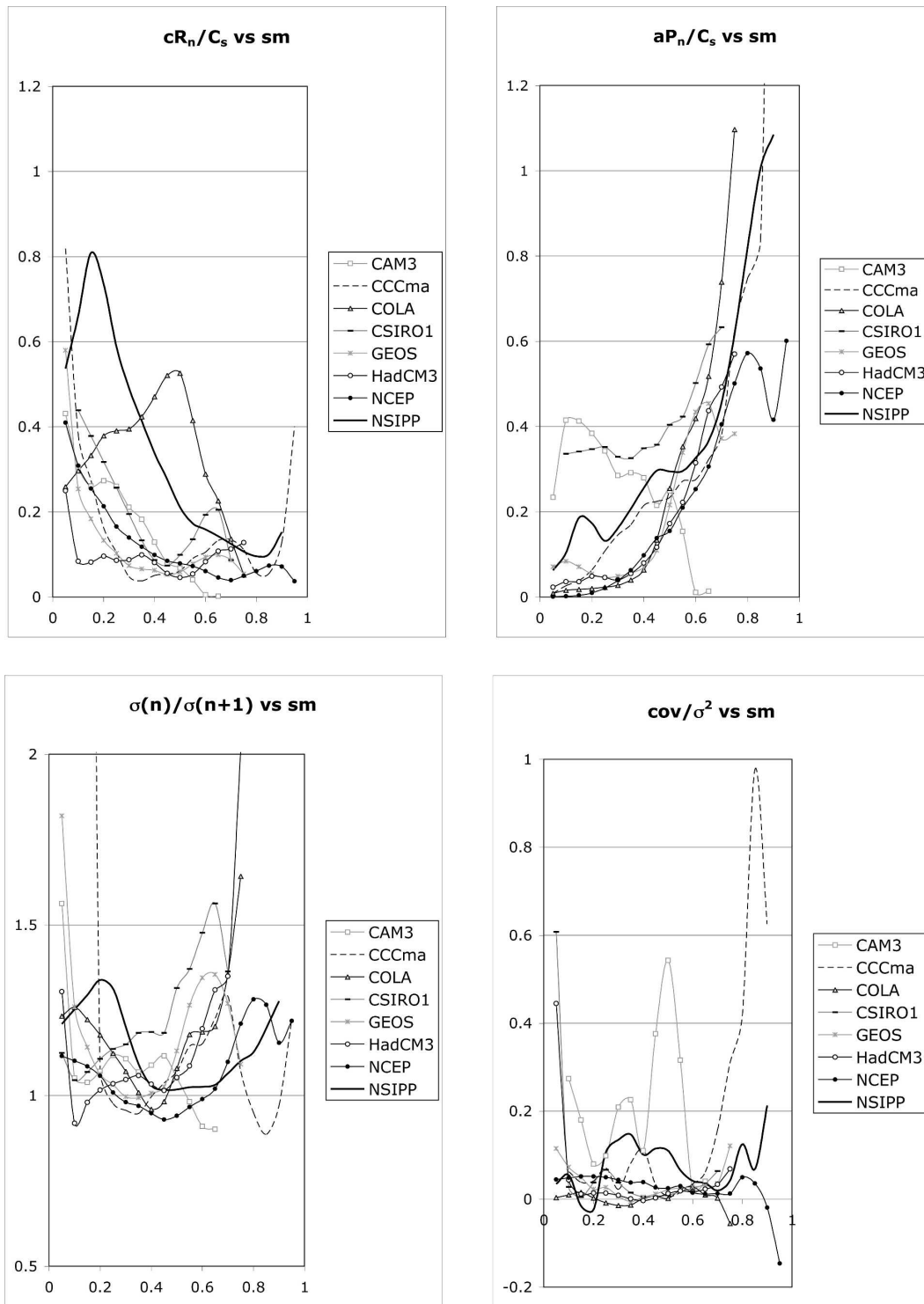


FIG. 13. Distribution of  $(c\bar{R}_n/C_s)$ ,  $(a\bar{P}_n/C_s)$ ,  $(\sigma_{w_n}/\sigma_{w_{n+1}})$ , and  $[\text{cov}(w_n, F_n)/\sigma_{w_n}^2]$  as functions of soil moisture (computed as bins for given soil moisture ranges).

sation of the effects of the other terms. Note that these compensating mechanisms at the low and high ends of soil wetness can be well understood if one considers the effects of the evaporation's and runoff's sensitivity

terms at those extremes. As discussed in section 2b, both terms induce reductions of initial soil moisture anomalies (thereby reducing soil moisture memory). Therefore, whenever these terms are large, they will

induce a reduction of variance during the time period  $(n, n + 1)$  and hence high values of  $(\sigma_{w_n}/\sigma_{w_{n+1}})$ . Figure 13 suggests that this effect is more important in determining the value of the seasonality term than possible reductions linked with increased forcing variance during the time period  $(n, n + 1)$  [e.g.,  $(\sigma_{w_n}/\sigma_{w_{n+1}}) < 1$ ; see Fig. 5 in KS01].

In summary, despite the spread among the AGCMs, this analysis shows that common features can be identified in the relationship between soil moisture memory and soil moisture regime. Soil moisture memory is lowest in humid areas, and also decreases at low soil moisture values. Its variations are mostly determined by the evaporation (dry regimes) and runoff (wet regimes) sensitivity terms, with some compensation effects by the seasonality and covariance terms. Overall, soil moisture memory is highest in regions of intermediate soil moisture, where both the evaporation and runoff sensitivity terms are small. Finally, the compensation mechanisms identified between the seasonality and the evaporation and runoff sensitivity terms are found to be important for extreme low and high values of soil wetness and suggest that soil moisture memory cannot be understood simply as a sum of the effects of the four terms of Eq. (4), but that interrelations between these terms also need to be taken into account.

## 7. Soil moisture memory and land–atmosphere coupling

A main motivation for investigating soil moisture memory characteristics across the globe is the possible use of soil moisture initialization for seasonal forecasting. The potential of soil moisture for seasonal forecasting is likely to be highest in regions where both soil moisture memory and land–atmosphere coupling are important. In this section, we very briefly investigate where such regions are likely to be located.

The yield of an estimate of land–atmosphere coupling across the globe was one of the main aims of the GLACE project (Koster et al. 2004a). Since these estimates are available for the simulations analyzed in this study, we can easily compare them with the average soil moisture memory of the AGCMs. Figure 14 displays in the top panel the average values of  $\Omega(P, S) - \Omega(P, W)$  for the eight models investigated here. For a detailed description of the  $\Omega$  parameter and the land–atmosphere coupling analysis of the GLACE simulations, please refer to Koster et al. (2004a, 2006) and Guo et al. (2006). For our present analysis, it suffices to see  $\Omega(P, S) - \Omega(P, W)$  as an estimate of the strength of land–atmosphere coupling in the AGCMs and how precipitation is impacted by this coupling. Note that the

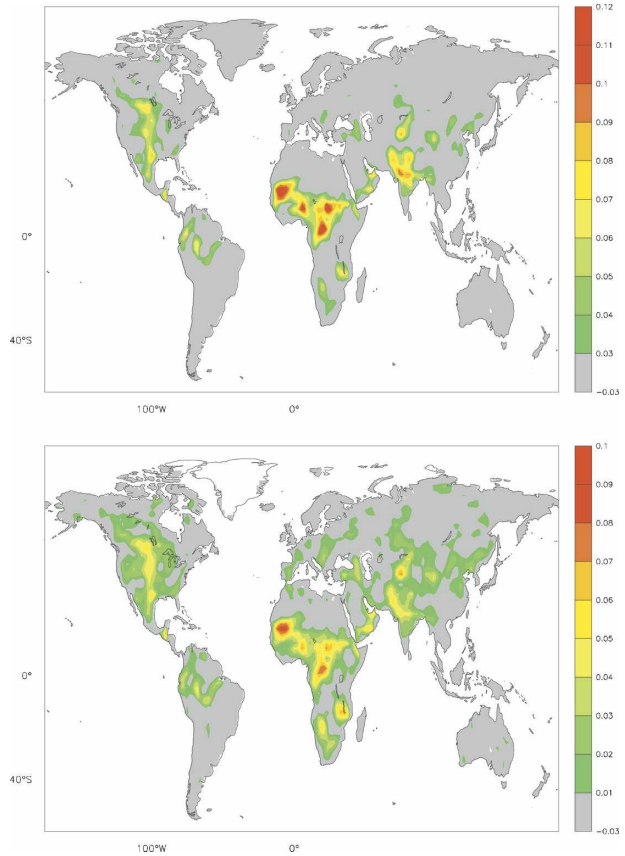


FIG. 14. (top) Mean  $\Omega(P, S) - \Omega(P, W)$  of the eight AGCMs investigated. (bottom) Mean  $\Omega(P, S) - \Omega(P, W)$  of the eight AGCMs multiplied by the average  $\rho_{27}$  values of the models.

average  $\Omega(P, S) - \Omega(P, W)$  obtained for the eight AGCMs analyzed here is very close to the values obtained for the whole set of GLACE simulations (12 in total; see Koster et al. 2006). This gives us thus some confidence that the subset of simulations considered in the present paper is representative of the whole GLACE ensemble. As discussed in Koster et al. (2004a, 2006), some regions of high land–atmosphere coupling (or “hot spots”) are easily recognizable from the average  $\Omega(P, S) - \Omega(P, W)$  values: the central Great Plains of North America (also NAMS region), northern India, the Sahel region, as well as equatorial Africa.

The bottom plot of Fig. 14 displays the quantity  $[\Omega(P, S) - \Omega(P, W)] * \rho_{27}$ . This can be considered as an estimate of the “seasonal forecasting potential,” or a combination of strong soil moisture memory and strong land–atmosphere coupling. Interestingly, though this picture is very similar to the one for  $\Omega(P, S) - \Omega(P, W)$  only, there are a few differences. In particular, while the formerly identified hot spots of land–atmosphere coupling are naturally again clearly highlighted, other regions appear to have both a combination of high soil

moisture memory and high land–atmosphere coupling: for instance the Mediterranean and Danube regions in Europe, which are known for a propensity to extended drought periods. Note as well that the hot spot regions do not all present the same soil moisture memory and thus potential for seasonal forecasting:  $[\Omega(P, S) - \Omega(P, W)] * \rho_{27}$  in the Sahel and equatorial Africa regions is about as high as in the Great Plains, while  $\Omega(P, S) - \Omega(P, W)$  was much higher in the former than in the latter. This thus confirms that the Great Plains of North America is a region with particularly high potential for using soil moisture initialization in seasonal forecasting (e.g., Koster et al. 2004b).

## 8. Summary and conclusions

In this study, we have investigated the (near) monthly soil moisture memory characteristics of eight AGCMs, utilizing simulations from the GLACE experiment. This survey is the first of its kind, in that it investigates global soil moisture memory for a range of AGCMs instead of focusing on a single-model analysis. The main value of such a multimodel analysis is that 1) it allows us to determine the extent to which previous results obtained in single-model analyses might apply to a larger number of models; 2) it can help identify causes for intermodel differences in memory behavior; and 3) averaging the memory results across a number of models provides an estimate of the global memory distribution (something that cannot be obtained from observations) that is much less affected by the model-dependent deficiencies or biases that weaken single-model analyses.

The results of this investigation show that the AGCMs present relatively similar global patterns of soil moisture memory. Outliers are generally characterized by anomalous water-holding capacity or biases in radiation forcing. Despite the range in the AGCMs' behavior, the average soil moisture memory characteristics of the models appear realistic when compared to available in situ soil moisture observations.

We use here the analysis framework proposed by KS01 for analyzing and identifying the main processes controlling soil moisture memory in the models. Equation (4) is obtained through a linearization of the dependency of the evaporation and runoff fractions on soil moisture. While this is of course an important simplification, the results of this multimodel analysis confirm previous results from KS01 and Mahanama and Koster (2003) demonstrating that (4) is a good approximation of simulated soil moisture memory. More detailed analyses comparing these results with, for example, stochastic–dynamical models (e.g., Laio et al.

2001; Porporato and D'Odorico 2004) lie outside the scope of the present study, but could offer useful perspectives for future studies.

The analysis of the four terms of (4) reveals that soil moisture memory in the models is mostly controlled by the evaporation ( $c\bar{R}_n/C_s$ ) and runoff ( $a\bar{P}_n/C_s$ ) sensitivity terms. For a majority of the AGCMs, soil moisture memory is controlled by ( $a\bar{P}_n/C_s$ ) in humid areas and by ( $c\bar{R}_n/C_s$ ) in dry areas. It is highest in regions of intermediate soil moisture content, where both terms are small. The seasonality term has less impact on the overall soil moisture memory, but is seen to partly compensate for the effects of these two terms, particularly in extreme dry and wet regimes. Land–atmosphere feedback is rarely large enough to affect overall soil moisture memory, except in regions with strong land–atmosphere coupling.

One should of course note a few caveats of our study. First, these results are derived for boreal summer only. The relative importance of the four terms is likely to vary over the course of the year. Second, the GLACE experiments analyzed here use a relatively quiescent (i.e., neither El Niño nor La Niña conditions) year for the prescription of global SSTs (see section 2a). In the Tropics, the impact of interannually varying SSTs on soil moisture memory can be particularly strong (Koster et al. 2000), and thus could also impact the values of the four terms, particularly the covariance term. Impacts in other regions cannot be excluded either. A third point is the fact that we focused on (near) monthly soil moisture autocorrelation, while it is possible that the relative strength of the controls described with (4) could be dependent upon the lag chosen. Such aspects could be the focus of future, more detailed studies on this issue.

Finally, our analysis shows that water-holding capacity is highly variable among the analyzed AGCMs and is the main factor responsible for intermodel differences in soil moisture memory. While the importance of the water-holding capacity for simulated soil moisture memory is not per se a surprising result (e.g., Delworth and Manabe 1988; Milly and Dunne 1994), of interest is the fact that the AGCMs utilize a wide variety of values for this parameter, with correspondingly strong impacts on simulated memory. This suggests that further research on this topic should first focus on the accurate determination of this parameter before complex process analyses can be performed with confidence, a fortiori when based on single-model experiments. Eventually, an improvement of the soil moisture and evaporation measurements' networks might help reduce the uncertainty still remaining among present AGCMs.

*Acknowledgments.* This research project was supported by an NCCR–Climate fellowship funded by the Swiss National Science Foundation. The individual AGCM contributions were supported by the participants' home institutions and funding agencies. We thank Sarith P. P. Mahanama and Michael Kistler for help with the observational datasets, as well as C. Adam Schlosser, Yogesh C. Sud, Ryan Teuling, and two anonymous reviewers for useful comments on the manuscript. The Ferret program ([www.ferret.noaa.gov](http://www.ferret.noaa.gov)) was used for the interpolation, analysis, and graphics in this paper.

## REFERENCES

- Albertson, J. D., and G. Kiely, 2001: On the structure of soil moisture time series in the context of land surface models. *J. Hydrol.*, **243**, 101–119.
- Bacmeister, J. T., P. J. Pegion, S. D. Schubert, and M. J. Suarez, 2000: Atlas of seasonal means simulated by the NSIPP1 atmospheric GCM. NASA Tech. Memo. 2000-104606, Vol. 17, 194 pp.
- Boer, G. J., N. A. McFarlane, and M. Lazare, 1992: Greenhouse gas-induced climate change simulated with the CCC second-generation general circulation model. *J. Climate*, **5**, 1045–1077.
- , —, and —, 1992: Greenhouse gas-induced climate change simulated with the CCC second-generation general circulation model. *J. Climate*, **5**, 1045–1077.
- Bonan, G. B., K. W. Oleson, M. Vertenstein, S. Levis, Z. Zeng, Y. Dai, R. E. Dickinson, and Z.-L. Yang, 2002: The land surface climatology of the Community Land Model coupled to the NCAR Community Climate Model. *J. Climate*, **15**, 3123–3149.
- Collins, W. D., and Coauthors, 2004: Description of the NCAR Community Atmosphere Model (CAM 3.0). NCAR Tech. Note NCAR/TN-464+STR, 214 pp. [Available online at <http://www.cesm.ucar.edu/models/atm-cam/docs/description/>.]
- Conaty, A. L., J. C. Jusem, L. Takacs, D. Keyser, and R. Atlas, 2001: The structure and evolution of extratropical cyclones, fronts, jet streams, and the tropopause in the GEOS general circulation model. *Bull. Amer. Meteor. Soc.*, **82**, 1853–1867.
- Cox, P. M., R. A. Betts, C. B. Bunton, R. L. H. Essery, P. R. Rowntree, and J. Smith, 1999: The impact of new land surface physics on the GCM simulation of climate and climate sensitivity. *Climate Dyn.*, **15**, 183–203.
- Delworth, T. L., and S. Manabe, 1988: The influence of potential evaporation on the variabilities of simulated soil wetness and climate. *J. Climate*, **1**, 523–547.
- Dirmeyer, P. A., and F. J. Zeng, 1999: An update to the distribution and treatment of vegetation and soil properties in SSiB. COLA Tech. Rep. 78, 25 pp. [Available from the Center for Ocean–Land–Atmosphere Studies, 4041 Powder Mill Road, Suite 302, Calverton, MD 20705.]
- Entin, J. K., A. Robock, K. Ya. Vinnikov, S. E. Hollinger, S. Liu, and A. Namkhai, 2000: Temporal and spatial scales of observed soil moisture variations in the extratropics. *J. Geophys. Res.*, **105** (D9), 11 865–11 877.
- Essery, R. L. H., M. J. Best, R. A. Betts, P. M. Cox, and C. M. Taylor, 2003: Explicit representation of subgrid heterogeneity in a GCM land surface scheme. *J. Hydrometeor.*, **4**, 530–543.
- Guo, Z.-C., and Coauthors, 2006: GLACE: The Global Land–Atmosphere Coupling Experiment. Part II: Analysis. *J. Hydrometeor.*, **7**, 611–625.
- Hirschi, M., S. I. Seneviratne, and C. Schär, 2006: Seasonal variations in terrestrial water storage for major midlatitude river basins. *J. Hydrometeor.*, **7**, 39–60.
- Hollinger, S. E., and S. A. Isard, 1994: A soil moisture climatology of Illinois. *J. Climate*, **4**, 822–833.
- Huffman, G. J., and Coauthors, 1997: The Global Precipitation Climatology Project (GPCP) Combined Precipitation Data Set. *Bull. Amer. Meteor. Soc.*, **78**, 5–20.
- Kalnay, E., and Coauthors, 1996: The NCEP/NCAR 40-Year Reanalysis Project. *Bull. Amer. Meteor. Soc.*, **77**, 437–471.
- Kinter, J. L., and Coauthors, 1997: Formulation. Vol. 1. The COLA atmosphere–biosphere general circulation model. COLA Tech. Rep. 51, 46 pp. [Available from the Center for Ocean–Land–Atmosphere Studies, 4041 Powder Mill Road, Suite 302, Calverton, MD 20705.]
- Koster, R. D., and M. J. Suarez, 1992: Modeling the land surface boundary in climate models as a composite of independent vegetation stands. *J. Geophys. Res.*, **97**, 2697–2716.
- , and —, 1996: Energy and water balance calculations in the Mosaic LSM. NASA Tech. Memo. 104606, Vol. 9, 59 pp. [Available from NASA Center for Aerospace Information, 800 Elkridge Landing Rd., Linthicum Heights, MD 21090-2934.]
- , and P. C. D. Milly, 1997: The interplay between transpiration and runoff formulations in land surface schemes used with atmospheric models. *J. Climate*, **10**, 1578–1591.
- , and M. J. Suarez, 2001: Soil moisture memory in climate models. *J. Hydrometeor.*, **2**, 558–570.
- , —, and M. Heiser, 2000: Variance and predictability of precipitation at seasonal-to-interannual timescales. *J. Hydrometeor.*, **1**, 26–46.
- , and Coauthors, 2004a: Regions of strong coupling between soil moisture and precipitation. *Science*, **305**, 1138–1140.
- , and Coauthors, 2004b: Realistic initialization of land surface states: Impacts on subseasonal forecast skill. *J. Hydrometeor.*, **5**, 1049–1063.
- , and Coauthors, 2006: GLACE: The Global Land–Atmosphere Coupling Experiment. Part I: Overview. *J. Hydrometeor.*, **7**, 590–610.
- Kowalczyk, E. A., J. R. Garratt, and P. B. Krummel, 1994: Implementation of a soil–canopy scheme into the CSIRO GCM—Regional aspects of the model response. CSIRO Atmospheric Research Tech. Paper 32, Aspendale, Australia, 59 pp.
- Laio, F., A. Porporato, L. Ridolfi, and I. Rodriguez-Iturbe, 2001: Plants in water-controlled ecosystems: Active role in hydrological processes and response to water stress. II. Probabilistic soil moisture dynamics. *Adv. Water Res.*, **24**, 707–723.
- Liu, Y., and R. Avissar, 1999a: A study of persistence in the land–atmosphere system using a general circulation model and observations. *J. Climate*, **12**, 2139–2153.
- , and —, 1999b: A study of persistence in the land–atmosphere system with a fourth-order analytical model. *J. Climate*, **12**, 2154–2167.
- Mahanama, S. P. P., and R. D. Koster, 2003: Intercomparison of soil moisture memory in two land surface models. *J. Hydrometeor.*, **4**, 1134–1146.
- , and —, 2005: AGCM biases in evaporation regime: Im-

- acts on soil moisture memory and land–atmosphere feedback. *J. Hydrometeorol.*, **6**, 656–669.
- McFarlane, N. A., G. J. Boer, J.-P. Blanchet, and M. Lazare, 1992: The Canadian Climate Centre second-generation general circulation model and its equilibrium climate. *J. Climate*, **5**, 1013–1044.
- McGregor, J. L., 1996: Semi-Lagrangian advection on conformal-cubic grids. *Mon. Wea. Rev.*, **124**, 1311–1322.
- , and M. R. Dix, 2001: The CSIRO conformal-cubic atmospheric GCM. *IUTAM Symposium on Advances in Mathematical Modeling of Atmosphere and Ocean Dynamics*, P. F. Hodnett, Ed., Kluwer, 197–202.
- Milly, P. C. D., and K. A. Dunne, 1994: Sensitivity of the global water cycle to the water-holding capacity of land. *J. Climate*, **7**, 506–526.
- Mocko, D. M., and Y. C. Sud, 2001: Refinements to SSiB with an emphasis on snow-physics: Evaluation and validation with GSWP and Valdai data. *Earth Interactions*, **5**. [Available online at <http://EarthInteractions.org>.]
- Moorthi, S., H.-L. Pan, and P. Caplan, 2001: Changes to the 2001 NCEP Operational MRF/AVN Global Analysis/Forecast System. NWS Technical Procedures Bulletin 484, 14 pp.
- Oleson, K. W., and Coauthors, 2004: Technical description of the Community Land Model (CLM). NCAR Tech. Note, NCAR/TN-461+STR, 174 pp. [Available online at <http://www.cesm.ucar.edu/models/ccsm3.0/clm3/index.html>.]
- Pan, H. L., and L. Mahrt, 1987: Interaction between soil hydrology and boundary-layer development. *Bound.-Layer Meteorol.*, **38**, 185–202.
- Pope, V. D., M. L. Gallani, P. R. Rowntree, and R. A. Stratton, 2000: The impact of new physical parameterizations in the Hadley Centre climate model: HadAM3. *Climate Dyn.*, **16**, 123–146.
- Porporato, A., and P. D’Odorico, 2004: Phase transitions driven by state-dependent Poisson noise. *Phys. Rev. Lett.*, **92**, 110601, doi:10.1103/PhysRevLett.92.110601.
- Robock, A., K. Y. Vinnikov, G. Srinivasan, J. K. Entin, S. E. Hollinger, N. A. Speranskaya, S. Liu, and A. Namkhai, 2000: The Global Soil Moisture Data Bank. *Bull. Amer. Meteor. Soc.*, **81**, 1281–1299.
- Rudolf, B., H. Hauschild, W. Reuth, and U. Schneider, 1994: Terrestrial precipitation analysis: Operational method and required density of point measurements. *Global Precipitation and Climate Change*, M. Desbois and P. Desalmond, Eds., NATO ASI Series I, Vol. 26, Springer-Verlag, 173–186.
- Schlosser, C. A., and P. C. D. Milly, 2002: A model-based investigation of soil moisture predictability and associated climate predictability. *J. Hydrometeorol.*, **3**, 483–501.
- Seneviratne, S. I., P. Viterbo, D. Lüthi, and C. Schär, 2004: Inferring changes in terrestrial water storage using ERA-40 reanalysis data: The Mississippi River basin. *J. Climate*, **17**, 2039–2057.
- Sud, Y. C., and G. K. Walker, 1999a: Microphysics of clouds with the relaxed Arakawa–Schubert Cumulus Scheme (McRAS). Part I: Design and evaluation with GATE Phase III data. *J. Atmos. Sci.*, **56**, 3221–3240.
- , and —, 1999b: Microphysics of clouds with the relaxed Arakawa–Schubert Cumulus Scheme (McRAS). Part II: Implementation and performance in GEOS II GCM. *J. Atmos. Sci.*, **56**, 3221–3240.
- Verseghy, D. L., 1991: CLASS—A Canadian land surface scheme for GCMs: I. Soil model. *Int. J. Climatol.*, **11**, 111–133.
- Vinnikov, K. Ya., and I. B. Yeserkepova, 1991: Empirical data and model results. *J. Climate*, **4**, 66–79.
- , A. Robock, N. A. Speranskaya, and A. Schlosser, 1996: Scales of temporal and spatial variability of midlatitude soil moisture. *J. Geophys. Res.*, **101** (D3), 7163–7174.
- Wu, W., and R. E. Dickinson, 2004: Time scales of layered soil moisture memory in the context of land–atmosphere interaction. *J. Climate*, **17**, 2752–2764.
- , M. A. Geller, and R. E. Dickinson, 2002: The response of soil moisture to long-term variability of precipitation. *J. Hydrometeorol.*, **3**, 604–613.
- Xue, Y., P. J. Sellers, J. L. Kinter, and J. Shukla, 1991: A simplified biosphere model for global climate studies. *J. Climate*, **4**, 345–364.
- Zhao, M., and P. Dirmeyer, 2003: Production and analysis of GSWP-2 near-surface meteorology data sets. COLA Tech. Rep. 159, 22 pp. [Available from the Center for Ocean–Land–Atmosphere Studies, 4041 Powder Mill Road, Suite 302, Calverton, MD 20705.]
- Zobler, L., 1986: A World Soil File for Global Climate Modelling. NASA Tech. Memo. 87802, NASA Goddard Institute for Space Studies, New York, NY, 32 pp.